The Potential Impact on Atmospheric Ozone and Temperature of Increasing Trace Gas Concentrations

GUY BRASSEUR[1]

National Center for Atmospheric Research, Boulder, Colorado

ANNE DE RUDDER

Belgian Institute for Space Aeronomy, Brussels, Belgium

The response of the atmosphere to emissions of chlorofluorocarbons (CFCs) and other chlorocarbons and to increasing concentrations of other radiatively active trace gases such as CO_2, CH_4, and N_2O is calculated by means of a coupled chemical-radiative-transport one-dimensional model. It is shown that significant reductions in the ozone concentration and in the temperature should be expected in the upper stratosphere as a result essentially of increasing concentrations of active chlorine produced by photo-decomposition of the CFCs. For a constant emission of chlorofluorocarbons-11 and -12 at approximately the 1980 level (309 kT/yr for F-11 and 433 kT/yr for F-12) the calculated decrease (assuming no other changes) in the ozone concentration relative to the preindustrial atmosphere is approximately 60–70% at 40 km, and the reduction in the ozone column is 8.7% when temperature feedback is included in the model and 5.5% when it is omitted. The model also shows that a doubling of CO_2 leads to a 1.8% increase in the ozone column abundance and a 2 K increase in the surface temperature. At 40 km the ozone density is enhanced by 15% and the temperature reduced by 8 K. A doubling of methane produces a 2.4% increase in the ozone column. A 20% enhancement in the nitrous oxide content leads to an ozone depletion of 1.4%. Time-dependent calculations of ozone and temperature show that if the production of F-11 and F-12 increases by 3%/yr until it reaches a capacity cap equal to 1.5 times the 1985 world production level, the maximum ozone depletion should be of the order of 4–5%, assuming a growth in the concentration of CO_2, CH_4, and N_2O of about 0.5, 1.0, and 0.25%/yr, respectively. For this scenario the maximum ozone depletion is found to occur in year 2070. The slight increase appearing after 2070 is directly dependent on the future growth in the methane concentration. If the production of F-11 and F-12 increases continuously by 3%/yr, without capacity cap, and if the changes in the concentration of other trace gases are ignored, the ozone column abundance is predicted to be reduced by more than 10% after year 2050. The model shows an almost linear relation between the ozone depletion and the chlorine content as long as the mixing ratio of active chlorine remains smaller than that of active nitrogen. The O_3/Cl_x sensitivity, however, is a strong function of NO_y content. For amounts of chlorine comparable or larger than those of active nitrogen the ozone depletion increases rapidly with the amount of chlorine present in the atmosphere.

1. INTRODUCTION

It is now well recognized that the increase in the concentration of trace gases in the atmosphere such as the chlorofluorocarbons (CFCs), nitrous oxide (N_2O), methane (CH_4), and carbon dioxide (CO_2), essentially as a result of agricultural practices and industrial activity, should significantly modify the structure of the ozone layer and influence the earth's climate in the future. Among the species which have the potential to perturb the ozone layer in the stratosphere, the chlorofluorocarbons play a major role. These organic molecules are used as aerosol propellants, refrigerants, foam-blowing agents, solvents, etc. Those which are important to the ozone issue are produced in relatively large quantity and are stable toward chemical destruction in the troposphere. The species involved are essentially $CFCl_3$ (F-11), CF_2Cl_2 (F-12). In addition, other important compounds are CCl_4 (carbon tetrachloride), CH_3CCl_3 (methyl chloroform), and to a lesser extent, $CF_2ClCFCl_2$ (F-113). Other potential harmful industrial halocarbons such as $CHClF_2$ (F-22), $CBrF_3$ (Halon 1301), or CF_2ClBr (Halon 1211) play at the present time only a secondary role and will not be considered further. The global emissions of F-11 and F-12 have increased by about 10%/yr until 1974. Since then the release in the atmosphere has been essentially constant, namely about 250–350 kT/yr for F-11 and 350–450 kT/yr for F-12 [*Chemical Manufacturers Association (CMA)*, 1985; *Fabian*, 1986]. However, as the lifetime of these two compounds is of the order of 80 years for F-11 and 170 years for F-12, their concentration in the stratosphere has continued to increase. Large uncertainties exist in the quantitative values associated with the budget of CCl_4. According to a recent study by *Simmonds et al.* [1983], the emission of carbon tetrachloride should be of the order of 100 kT/yr and its global lifetime close to 75 years. The emission rate of methyl chloroform in the atmosphere (expressed in mass units) appears to be more than twice that of F-11 and F-12 and is growing by about 16%/yr [*Fabian*, 1986]. However, according to *Logan et al.* [1981], about 70% of the sink of this gas (essentially by OH) takes place in the troposphere, so that the lifetime of CH_3CCl_3 is of the order of 7 years [*Rasmussen and Khalil*, 1981a].

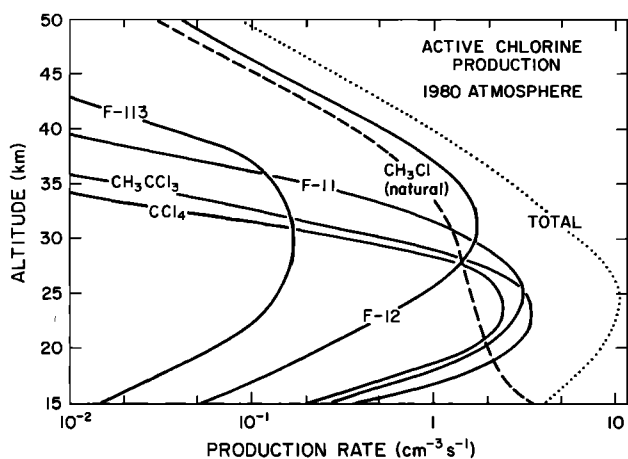The only important natural source of chlorine atoms appears to be through methyl chloride (CH_3Cl), which is pro-

Fig. 1. Contribution of natural CH_3Cl and man-made chlorocarbons to the production rate of active chlorine in the stratosphere (1980 reference atmosphere).

duced by the oceans, by biomass burning, and by fungi [*Harper*, 1985]. A range of 1350–9000 kT/yr is quoted by *Fabian* [1986], based on estimates by *Cicerone et al.* [1975], *Yung et al.* [1975], *Singh et al.* [1979], *Graedel* [1979], and *Crutzen et al.* [1979]. Figure 1 shows the contribution of the various organic chlorine compounds to the production rate of inorganic chlorine for conditions corresponding to year 1980. The chlorine atoms resulting from the dissociation of the chlorocarbons (ClCs) destroy ozone through the catalytical cycle [*Stolarski and Cicerone*, 1974]

$$Cl + O_3 \rightarrow ClO + O_2$$
$$ClO + O \rightarrow Cl + O_2 \qquad (1)$$
$$\text{net:} \quad \overline{O + O_3 \rightarrow 2O_2}$$
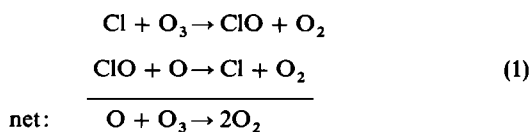
In the preindustrial atmosphere the mixing ratio of total inorganic chlorine (essentially in the form of Cl, ClO, $ClONO_2$, HCl, and HOCl) was close to 0.7 parts per billion by volume (ppbv), as a result of the destruction of the naturally produced methyl chloride. It is presently of the order of 2.5–2.8 ppbv in the upper stratosphere [*World Meteorological Organization* (*WMO*)/*National Aeronautics and Space Administration* (*NASA*), 1986].

Nitrous oxide (N_2O), which has a current surface mixing ratio of 307 ppbv [*Rasmussen and Khalil*, 1986], is the main source of nitrogen oxides in the stratosphere. It is produced by biological processes, mostly by bacterial nitrification and denitrification, and by fossil fuel and biomass combustion. Its growing concentration (annually, about 0.2–0.3%; *Weiss* [1981], *Khalil and Rasmussen* [1983], and *Rasmussen and Khalil* [1986]) is believed to be largely associated with human activity. Nitric oxide resulting from its destruction by electronically excited oxygen atoms [*Nicolet*, 1971; *Crutzen*, 1971] is responsible for what is known to be the most efficient ozone destruction mechanism in the stratosphere [*Crutzen*, 1970] by the following catalytical cycle

$$NO + O_3 \rightarrow NO_2 + O_2$$
$$NO_2 + O \rightarrow NO + O_2 \qquad (2)$$
$$\text{net:} \quad \overline{O + O_3 \rightarrow 2O_2}$$
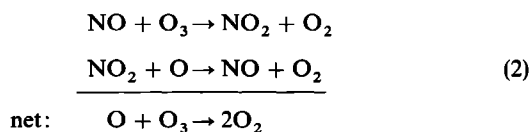
Methane (CH_4) is the most abundant hydrocarbon in the atmosphere. Its present mixing ratio at the surface is about 1.7 parts per million by volume (ppmv) in the northern hemisphere [*Rasmussen and Khalil*, 1986; *WMO/NASA*, 1986]. A substantial increase in the concentration of this gas has been observed by *Rasmussen and Khalil* [1981b] [$(2 \pm 0.5)\%$/yr], by *Blake et al.* [1982] [$1.5 \pm 0.5\%$/yr], and by *Rasmussen and Khalil* [1986] [(17.5 ± 1.3) parts per trillion by volume (pptv)/yr]. This molecule initiates a complex chemistry which is capable of altering the concentration of other radiatively active trace gases. For example, the oxidation of methane produces, when the amount of nitrogen oxides is sufficiently large, ozone molecules, especially in the troposphere [*Crutzen*, 1974, 1986]. Moreover, one of the end products of this oxidation chain is water vapor which is also radiatively active. The increase in the methane content should also modify the distribution of hydroxyl radicals with subsequent effects on the chemistry of other species. Such perturbations of OH should modify the photooxidation rates of several natural and anthropogenic species and affect the lifetime of trace gases that pass from the earth's surface to the troposphere and the stratosphere [*Thompson and Cicerone*, 1986]. Finally, the ratio between the concentration of ClO (which directly affects ozone) and HCl (which is a chlorine reservoir without chemical influence on ozone) is significantly affected by the methane content.

Carbon dioxide is chemically very stable in the entire atmosphere below 80-km altitude. Its mixing ratio is thus essen-

TABLE 1. Main Characteristics of the Chemical Species Involved in the Present Study (Source Gases Only) 1980 Conditions

Species	Typical Mixing Ratio at the Surface	Integrated Concentration Above the Surface, cm^{-2}	Total Atmospheric Mass, MT	Total Annual Destruction, kT/yr	Calculated Lifetime, years	Recent Growth Rate, %/yr
CO_2	340 ppmv	6.1×10^{21}	2.1×10^6	...	...	0.2–0.5
CH_4	1.6 ppmv	3.0×10^{19}	4183	6.38×10^5	6.5	1–2
N_2O	300 ppbv	5.8×10^{18}	2170	1.22×10^4	177	0.25
CH_3Cl	700 pptv	1.2×10^{16}	5.27	5.38	1	...
CCl_4	100 pptv	1.9×10^{15}	2.44	35	69	0–3
CH_3CCl_3	100 pptv	1.8×10^{15}	2.09	480	4	5–8
F-11	170 pptv	3.2×10^{15}	3.74	42.6	88	5–8
F-12	285 pptv	5.5×10^{15}	5.65	33.9	167	5–8
F-113	22 pptv	4.2×10^{14}	0.67	4.99	134	15–20

tially uniform below this level with a current value close to 350 ppmv. Continuous monitoring of the CO_2 concentration [*Keeling*, 1983] has shown an increase since 1958 of the order of 0.2–0.3%/yr, probably resulting in large part from combustion processes (coal, oil, natural gas) and land use changes (deforestation, burning, etc.). Table 1 summarizes the characteristics of the trace gases with potentially important chemical, radiative, and climatic effects, which are considered in the present study.

Model calculations reported, for example, in the *WMO/NASA* [1986] report predict a steady state ozone depletion of 5–9% for a constant anthropogenic production of (CICs) at the present level and neglecting the effect of increasing concentrations of other trace gases such as CO_2, CH_4, and N_2O. Moreover, as noted recently by *Ramanathan et al.* [1985] and by *Dickinson and Cicerone* [1986], the continuous additions of trace species during the next 65 years are predicted to cause the global surface temperature to rise by between 1 and 5 K.

Predictions of future changes in atmospheric ozone and temperature require coupled models which simultaneously and interactively represent the chemical and the radiative behavior of the atmosphere and its response to human perturbations. The purpose of this paper is to investigate these effects. The response of the atmosphere to the emissions of trace gases has been extensively studied in recent years [see, e.g., *Wang et al.*, 1976, 1986; *Wang and Molnar*, 1985; *Ramanathan*, 1976; *Ramanathan et al.*, 1985, 1987; *Donner and Ramanathan*, 1980; *Lacis et al.*, 1981; *Wuebbles*, 1983; *Callis et al.*, 1983; *Wuebbles et al.*, 1983; *Brasseur*, 1984; *Brasseur et al.*, 1985; *de Rudder and Brasseur*, 1985; *Bruehl and Crutzen*, 1984;

Owens et al., 1985; *Solomon et al.*, 1985; *Isaksen and Stordal*, 1986; *Dickinson and Cicerone*, 1986; *Connell and Wuebbles*, 1986; *Tricot and Berger*, 1987; and others]. Some of these papers have either studied the chemical sensitivity of ozone to changes in the amount of injected "source gases" (parameterizing crudely the radiative feedbacks and, in certain cases, ignoring the climatic impact at the earth's surface) or considered the pure radiative and climatic response of the injection in the atmosphere of "greenhouse gases" (neglecting chemical feedbacks). In this work all effects will be treated interactively through a coupled one-dimensional time-dependent chemical-radiative-transport model. This model, which is described in secton 2, is used (section 3) to predict future changes in the ozone content and in the temperature, based on several possible time-dependent scenarios of future atmospheric emissions. The sensitivity of the atmospheric responses to the values adopted for parameters such as the eddy diffusion coefficient for vertical transport and the atmospheric budget of nitrogen oxides is estimated and discussed in section 4.

2. MODEL

2.1. Model Description

The model used in the present study is one-dimensional and extends from the earth's surface to the altitude of 100 km, although the temperature is calculated only up to 60 km and kept fixed above 70 km (with a linear transition between 60 and 70 km). The vertical distribution of the trace gases is calculated by solving continuity/transport equations

$$\frac{\partial X_i}{\partial t} - \frac{1}{[M]} \frac{\partial}{\partial z}\left(K[M] \frac{\partial X_i}{\partial z}\right) = S_i \tag{3}$$

with appropriate boundary conditions. In this expression, X_i is the volume mixing ratio of species i, $[M]$ the atmospheric density, t the time, and z the altitude. The vertical eddy diffusion coefficient K parameterizes the strength of the net vertical exchanges. Its value is of the order of $(1–2) \times 10^5$ cm^2 s^{-1} in the troposphere and $(0.5–5) \times 10^4$ cm^2 s^{-1} in the stratosphere. The profile adopted in most numerical simulations in this work is identical to the profile used by D. J. Wuebbles (private communication, 1985) and is shown in Figure 2. The source term S_i is estimated, taking into consideration the formation and the destruction of each species i by chemical and photochemical reactions.

In order to avoid numerical problems due to the "stiffness" of the system of equations due to the very broad spectrum of lifetimes associated with the different chemical constituents, some of the species with strong chemical couplings are grouped, and (1) is applied to the "chemical family" as a whole instead of to each individual constituent. For the most reactive compounds, photochemical equilibrium conditions are applied. The system is then solved for the species belonging to the oxygen-hydrogen-carbon-nitrogen-chlorine families, using an implicit numerical method. The adopted boundary conditions applied for the 1980 reference atmosphere are identical to the conditions used in the *WMO/NASA* [1986] report and are specified in Table 2. For perturbed cases the boundary conditions of source gases are adapted to account for increasing mixing ratios or fluxes at the surface. Concentrations of ozone and nitrogen oxides are allowed to vary in the troposphere since a deposition velocity is specified for these species
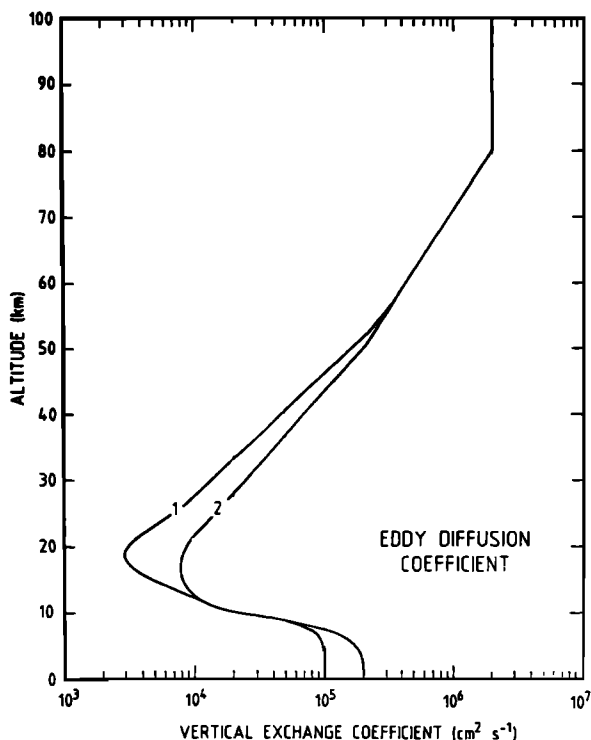

Fig. 2. Vertical distribution of eddy diffusion coefficients. Profile 1 (D. J. Wuebbles, private communication, 1985) is used in all model calculations unless otherwise specified. Profile 2 is considered only for sensitivity purposes.

TABLE 2. Boundary Conditions Adopted in the Model to
Describe the 1980 Atmosphere

Species	Lower Boundary	Upper Boundary
N_2O	$X = 300$ ppbv	$\Phi = 0$
CH_4	$X = 1.6$ ppmv	$\Phi = 0$
CH_3Cl	$X = 700$ pptv	$\Phi = 0$
CCl_4	$X = 100$ pptv	$\Phi = 0$
$CFCl_3$ (F-11)	$X = 170$ pptv	$\Phi = 0$
CF_2Cl_2 (F-12)	$X = 290$ pptv	$\Phi = 0$
$CF_2Cl\text{-}CFCl_2$ (F-113)	$X = 22$ pptv	$\Phi = 0$
CH_3CCl_3	$X = 100$ pptv	$\Phi = 0$
CO	$X = 100$ ppbv	$\Phi = 0$
Cl_x	$X = 1$ ppbv	$\Phi = 0$
NO_y	$w_D = -0.5$ cm/s	$X = 5.4$ ppbv
O_x	$w_D = -0.1$ cm/s	$X = 5.3 \times 10^{-2}$
H	$X = 0$	$X = 4.3$ ppbv

X is the mixing ratio, Φ is the vertical flux, and w_D is the deposition velocity.

at the lower boundary. The chemical rate constants required to calculate the source terms are taken from the Jet Propulsion Laboratory compilation [DeMore et al., 1985]. The photodissociation frequency of the molecules is calculated with the solar irradiance compiled by Brasseur and Simon [1981]. The solar penetration in the region of the Schumann-Runge bands of molecular oxygen, as well as the photodissociation rate of O_2 in the same spectral range, are derived using the method of Kockarts [1976]. The photodissociation coefficient of NO is calculated with the formula of Nicolet [1979]. The absorption cross sections of O_2 in the Herzberg continuum are taken from the in situ measurements by Herman and Mentall [1982]. The diurnal average of the photodissociaton coefficient is approximated by a four-point integral between sunrise and sunset [see Cunnold et al., 1975]. The water vapor mixing ratio in the stratosphere is specified such that the mixing ratio of hydrogen contained in H_2O, CH_4, and H_2 is constant with altitude. The water vapor profile is thus changing as the methane distribution is modified.

The code used to calculate the vertical distribution of the temperature has been developed by Ramanathan [1976], Donner and Ramanathan [1980], and Kiehl and Ramanathan [1983] and modified by Bruehl [1986]. It has been recently used by Bruehl and Crutzen [1984] to investigate the effects of greenhouse gases on atmospheric ozone and temperature.

The calculated heating rate resulting from the absorption of solar radiation involves the effect of ozone, nitrogen oxide, water vapor, and carbon dioxide. The heating by ozone and nitrogen dioxide is obtained from a detailed spectral integration involving the relevant absorption cross sections and solar irradiance. The heating by water vapor in the stratosphere is calculated according to the unpublished method of Ramanathan [see Bruehl, 1986]. The contribution of the heating by CO_2 is derived from a computation based on the broadband absorptance method expressed by Kiehl et al. [1985] for the 1.4-, 1.6-, 2.7-, and 4.3-μm bands. A total of 30 bands are included, based on the measurements of Yamanouchi [1977].

The radiative effect of the 15-μm band of CO_2 is estimated by the broadband model of Kiehl and Ramanathan [1983]. Total overlap is assumed for 56 "hot" and isotopic bands. In the upper stratosphere the transition from the Lorentz to the Doppler regime is performed by choosing the maximum cooling associated with these two line shapes [Ramanathan, 1976].

The temperature dependence of the line parameters is fully included. A broadband absorptance model with the related parameters specified by Ramanathan and Dickinson [1979] is adopted for the two bands of ozone near 9.6 μm. Again, the maximum cooling method is used to discriminate between Lorentz and Doppler regimes in the upper stratosphere. For water vapor the contribution of the vibration-rotation and pure rotation spectra is represented by the emissivity method of Ramanathan [1976], supplemented by data of Rogers and Walshaw [1966]. The fit of Roberts et al. [1976] is used for the water vapor continuum. Its contribution, however, is neglected in the stratosphere.

The broadband absorptance method of Ramanathan is used for methane and nitrous oxide with the data of Donner and Ramanathan [1980]. In the case of the N_2O band at 16.9 μm, two "hot" bands are considered simultaneously with the fundamental band. The overlap with the CO_2 and the H_2O spectra is treated as in the work by Kiehl and Ramanathan [1983]. For the 7.7 μm fundamental and hot bands the intensities are taken from McClatchey et al. [1973]. Overlap with H_2O and CH_4 bands as well as temperature dependences of the spectral parameters are fully included. The radiative transfer associated with the F-11 and F-12 molecules includes four bands for each constituent with intensities and bandwidths taken from Kagann et al. [1983].

This model, called code C1, is run iteratively until radiative equilibrium conditions are reached in the stratosphere. In the troposphere a convective adjustment is performed such that the lapse rate never exceeds −5.9 K/km. The surface temperature is obtained by an iterative procedure until an energy balance between incoming and outgoing radiation is acheived at the top of the atmosphere. Clouds are included with a top altitude of 4 km and a global coverage equal to 55% of the earth's area. For the 1980 atmosphere, in which the chemistry is self-consistently calculated, the surface temperature calculated in the model is 288.9 K. The incoming solar energy is 341.65 Wm^{-2}, and the outgoing shortwave energy is 109.28 Wm^{-2}, corresponding thus to a planetary albedo of 32%.

It should be noted that the interaction between the atmosphere and the ocean is not included in the radiative code. Because of its large heat capacity the ocean delays significantly the response of the surface temperature to perturbations in the concentration of precursor gases. Models, which intend to simulate explicitly the transient response of the earth's climate, usually consider three or more thermal reservoirs (for example, the atmosphere, the surface mixed layer of the ocean, and the deep ocean) and parameterize the heat transfer between these reservoirs [see, e.g., Dickinson, 1981]. Therefore changes in the surface temperature will be assessed only for steady state cases. Time history of the temperature will be reported only above 20 km, where the effect of the thermal inertia provided by the ocean is small.

In order to investigate the dependence of the results on the adopted radiative scheme, some of the calculations to derive the vertical temperature profile have been repeated using another numerical code (called C2). In this second model, which was used in the earlier work of Brasseur et al. [1985], the heating rate is calculated according to the formulation of Schoeberl and Strobel [1978]. The infrared code (J. J. Morcrette, private communication, 1983) derives average parameterized transmission functions for four broad wavelength intervals (15-μm CO_2, 9.6-μm O_3, rotational, and 6.3-μm H_2O
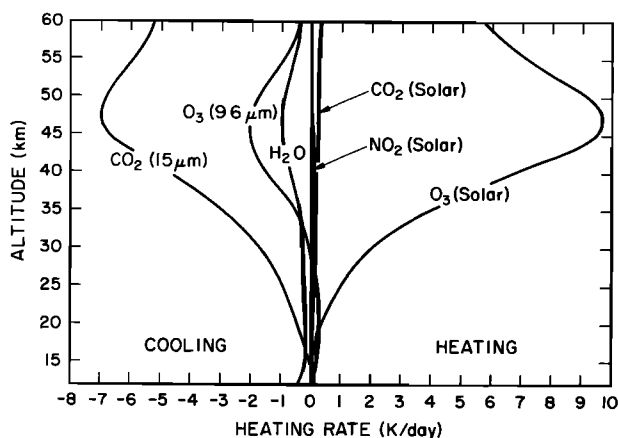
Fig. 3. Contribution of different trace gases to the heating by shortwave solar radiation and cooling by longwave terrestrial radiation of the atmosphere between 12- and 60-km altitude. The contribution of CH_4, N_2O, and the CFCs is too small to be visible on the figure.

bands and the atmospheric window) and takes into account the overlapping of several bands as well as the temperature and pressure effects on the spectral parameters. This parameterization of the transmission functions is based on a more detailed model including 116 intervals. The radiative effects of trace gases other than O_3, H_2O, and CO_2 are not included. A more detailed description of the radiative transfer code is given by Brasseur et al. [1985]. The vertical exchanges of heat are parameterized using a first-order closure scheme with an eddy thermal diffusion coefficient [Liou and Ou, 1983]. This coefficient is largest in the troposphere, where convective instability occurs, and is several orders of magnitude smaller in the stratosphere, where radiative equilibrium conditions are almost achieved. With values of the eddy thermal diffusion equal to 1.2 times the value of the exchange coefficient used for the vertical transport of the chemical species, the temperature profile is in reasonably good agreement with average observed values. Calculations with this code are performed for a global cloud cover of 50% and a top altitude of 5 km. A fixed relative (rather than absolute) humidity in the troposphere is adopted following Manabe and Wetherald [1967]. When perturbation calculations are performed, the surface temperature in this model is kept fixed. This should not significantly affect the calculated temperature changes in the upper stratosphere where radiative equilibrium is achieved but could introduce some errors in the temperature of the lower stratosphere, where the radiative lifetime is significantly longer.

2.2. Model Results for the Reference Atmosphere (1980)

Some of the model results for the 1980 reference atmosphere will now be presented in order to validate the model and to point out some unresolved questions in the chemistry of the stratosphere. Figure 3 shows the different components of the heating rate (solar radiation) and the cooling rate (terrestrial radiation) calculated by model C1. The largest contribution for the heating arises from ozone with a maximum of the order of 10 K/day near the stratopause. This effect is almost entirely balanced by the cooling resulting from the infrared emissions by CO_2, O_3, and H_2O. In the lower stratosphere all

contributions are significantly smaller so that the radiative lifetime becomes considerably longer. This lifetime has been estimated by Brasseur et al. [1987] to be 3 days at 50 km, 9 days at 40 km, and 17 days at 30 km. Gille and Lyjak [1986], from an analysis of the Limb Infrared Monitor of the Stratosphere (LIMS) data (observations taken from the Nimbus 7 satellite), have derived radiative relaxation times of 8 days at 40 km, 22 days at 30 km, 40 days at 25 km, and about 90 days at 20 km.

The assumption of radiative equilibrium in the lower stratosphere, made in all radiative-convective models (including C1), is approximate and introduces a severe limitation in these types of models. In fact, around and especially just above the tropopause, heat may be transported either horizontally or vertically. Such processes, however, can only be correctly treated in multidimensional models with a detailed description of the dynamics near the tropopause. The response of the temperature and, consequently, of ozone (as its chemistry is temperature dependent) in the lower stratosphere, derived by purely radiative models, might be inaccurate as the dynamical effects are not taken into account. In models such as C2 some vertical transport of heat is possible through eddy diffusion processes. However, it is not known how the exchange coefficients are affected by the perturbations (dynamical feedback) to be considered later in this paper.

The vertical profiles of the temperature obtained by both models with the same chemical composition are shown in Figure 4. Despite the numerous differences between these two models, the results are both in fairly good agreement with the U.S. Standard Atmosphere [1976]. In the lower stratosphere, however, the profiles are significantly different. Indeed, with the formulation of code C1, the transtion between the radiative and the convective regimes is sharp. In code C2 the diffusive formulation produces a much smoother transition between the troposphere and the stratosphere and a higher temperature minimum.

The vertical distribution of some of the source gases which are radiatively active is shown in Figures 5a and 5b. These profiles are calculated by the model (including temperature feedback with code C1), using the boundary conditions representative of 1980 conditions. When compared to observations [see WMO/NASA, 1986], the distribution of N_2O is in good
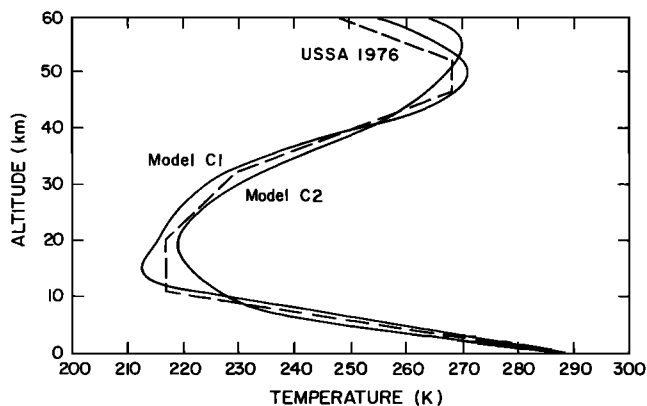

Fig. 4. Vertical distribution, between 0 and 60 km, of the temperature calculated by two different radiative codes (C1 and C2) and compared to the mean temperature profile of the U.S. standard atmosphere (1976).
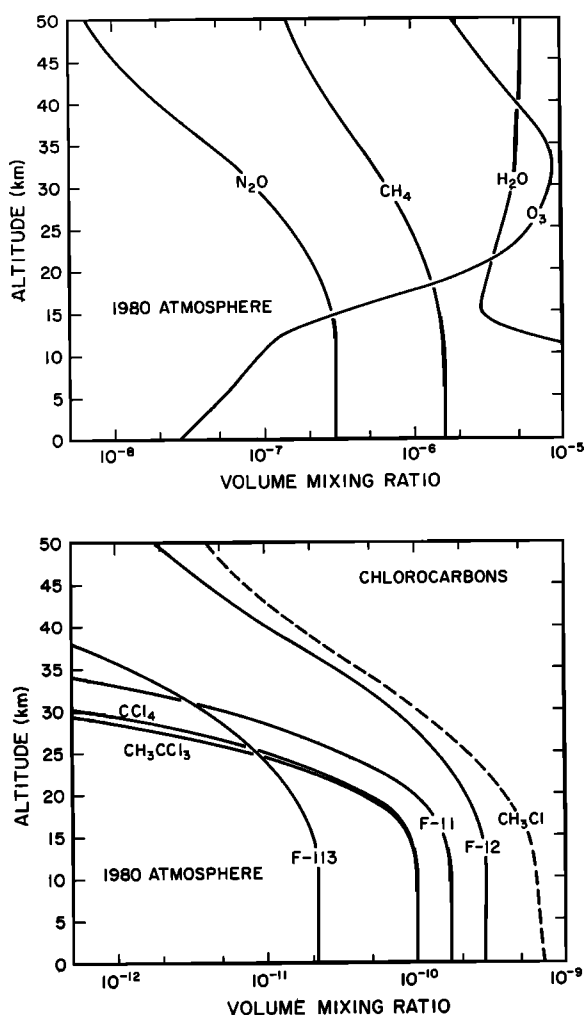
Fig. 5. Vertical distribution, between 0 and 50 km, of the mixing ratio of radiatively active gases, as computed by the one-dimensional model for 1980 conditions. Among the chlorocarbons, only F-11 and F-12 are included in the infrared code (Cl).

The vertical distribution of the ozone mixing ratio is represented in Figure 6. When compared wth observed data [*WMO/NASA*, 1986] this curve provides concentration values which are 20–30% lower than the measured values in the photochemically controlled region between 35 and 50 km. The possible causes for this discrepancy, which are discussed in detail in the *WMO/NASA* [1986] report, could be associated either with uncertainties in some rate constants of the HO_x or NO_x chemical schemes or with missing chemistry. The concentrations calculated in the lower stratosphere should be considered as approximate average values since a more realistic representation requires a multidimensional calculation involving a detailed dynamical representation. Indeed, in this region of the atmosphere the chemical lifetime of ozone exceeds the dynamical lifetime, so that the transport associated especially with planetary waves plays a dominant role.

As will be discussed below, the chemical balance of ozone and thus its sensitivity to perturbations by chemical compounds released in the atmosphere depend directly on the amount of the total number of active nitrogen atoms (NO_y = $NO + NO_2 + NO_3 + 2N_2O_5 + ClONO_2 + HNO_3 + HNO_4$) and of active chlorine atoms ($Cl_x = Cl + ClO + HCl + ClONO_2 + HOCl$) which are present in the atmosphere. The modeled vertical distributions of NO_y and Cl_x for 1980 conditions are displayed in Figure 7. The model provides a mixing ratio for NO_y which reaches a maximum of 17.4 ppbv at 33 km. This value is in good agreement with other one-dimensional models but is 30–50% lower than the maximum value deduced from the LIMS data (Nimbus 7 satellite) by *Callis et al.* [1985]. *Ko et al.* [1986] have shown recently, on a basis of a two-dimensional model, that upward transport of nitrogen oxides produced by lightning in the tropical troposphere (~ 2–4 10^6 t N/yr) could significantly enhance the con-

agreement with most data observed by in situ techniques. In the case of methane, the theoretical curve fits the measurements based on infrared absorption techniques by *Ackerman et al.* [1978] but is in disagreement (factor 2 at 40 km) with the values derived from the observations by the SAMS instrument on board the Nimbus 7 satellite [*Jones and Pyle*, 1984]. For the chlorocarbons the agreement between theory and observations is reasonably good in the case of F-12 and F-113, but the mixing ratios provided by the model above 20-km altitude are higher (factor 3 at 25 km) than the in situ observations for F-11. The same is true for CCl_4 and CH_3CCl_3. Similar disagreements are found in essentially all other one-dimensional models [see *WMO/NASA*, 1986], indicating that either all destruction processes of some halocarbons have not yet been identified or that the vertical transport of these species is not sufficiently well parameterized. *Holton* [1986] has shown recently that a proper one-dimensional representation of the vertical exchanges of chemical species requires for each constituent an eddy diffusion coefficient depending on the chemical lifetime of this particular species. In this work, as in all other models presently available, the same eddy diffusion profile has been used for all species (Figure 2). This question should be addressed in the future.
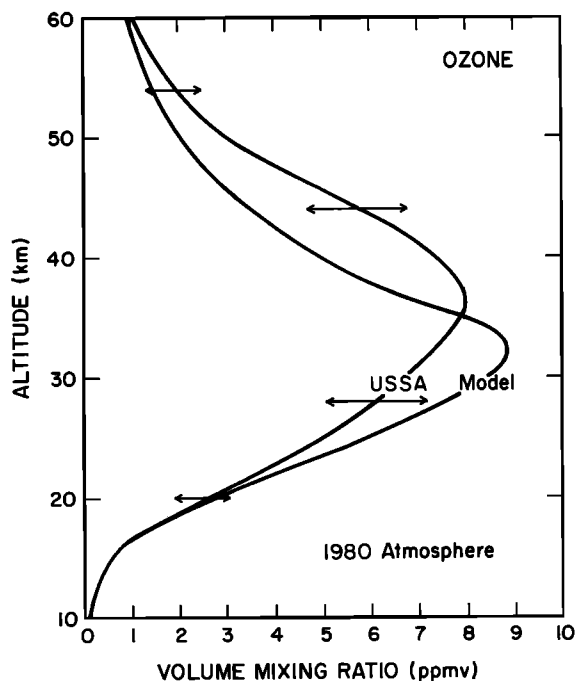

Fig. 6. Vertical distribution between 10 and 60 km of the ozone mixing ratio calculated by the model for 1980 conditions and compared to the mean ozone profile of the U.S. standard atmosphere (1976).
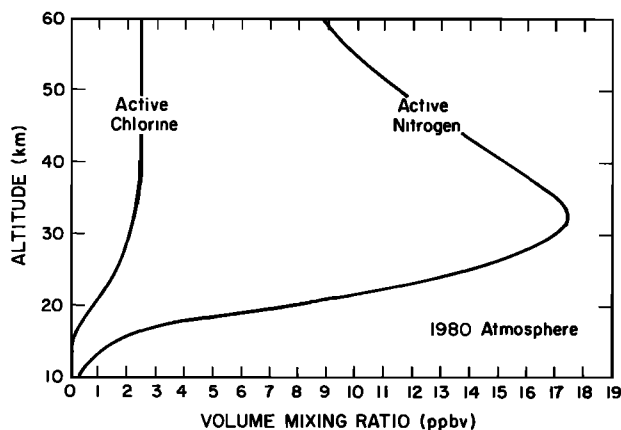
Fig. 7. Vertical distribution between 10 and 60 km of the active chlorine ($Cl + ClO + HCl + ClONO_2 + HOCl$) and of active nitrogen ($NO + NO_2 + NO_3 + 2N_2O_5 + HNO_3 + HNO_4 + ClONO_2$), calculated for 1980 conditions.

centration of NO_y in the stratosphere. In this model a production of 1×10^6 t N/yr has been assumed to be uniformly distributed between the surface and 10-km altitude. In the case of Cl_x, a mixing ratio of 2.4 ppbv is obtained at 50 km. This value is close to the mixing ratio determined by P. S. Connell (preprint, 1986) but is slightly smaller than what seems to result from the observation of the different species belonging to the Cl_x family and, in particular, of its most abundant constituent, namely HCl.

In conclusion, although the agreement between observed and calculated distributions of trace species is fairly good for a number of chemical constituents, some discrepancies, which have been pointed out, appear in certain altitude ranges of the atmosphere. The reason for these differences is not yet clear and could be attributed to an inadequate representation of the vertical transport, to errors in the values of the chemical and photochemical parameters, and/or to missing chemistry. These unresolved problems introduce some uncertainties in the quantitative predictions of future ozone and temperature changes provided by the current models used for these predictions.

3. RESPONSE OF THE ATMOSPHERE TO PRESCRIBED PERTURBATIONS

3.1. Steady State Calculations

In order to understand the physical and chemical processes involved in the response of the climatic system to chemical emissions in the atmosphere, single perturbations of each trace gas in isolation will first be considered. The variation in the

TABLE 3. Temperature Changes (in Degrees Kelvin) at the Surface for Different Perturbations

Perturbation	No Chemical Feedback	With Chemical Feedback
$CO_2 \times 2.0$	2.07	1.99
$CH_4 \times 2.0$	0.24	0.38
$N_2O \times 1.2$	0.06	0.06
$CFC \times 7.5$	0.60	0.40
Combined	2.91	2.71
$N_2O \times 2.0$	0.37	0.27

surface temperature resulting from the increase in the amount of greenhouse gases and obtained by a pure radiative model is compared in Table 3 to similar calculations in which the concentration of all species is allowed to vary as a result of chemical and photochemical reactions. The first case is referred to as a pure radiative model and the second as a calculation including chemical feedbacks. Differences are significant for some perturbation gases which significantly influence ozone such as methane and the chlorofluorocarbons. The inclusion of a detailed chemical code in radiative convective model appears thus to be important for studying the climatic impact of some trace gases. *Owens et al.* [1985] have also estimated the effect of chemical feedback on the calculated changes of surface temperature. Their study, consistently with ours, suggest very little change for the CO_2 perturbation case and show that the surface warming due to CH_4 is amplified when chemical feedback is included. However, at variance with the present study the calculations by Owens et al. indicate that the warming due to increasing concentrations of CFCs is somewhat larger when chemical feedback is included. The results reported in Table 3 are, however, generally in good agreement with other model calculations. For example, for a doubling in CO_2 the temperature increase derived by *Donner and Ramanathan* [1980], *Lacis et al.* [1981], *Owens et al.* [1985], and *Wang and Molnar* [1985] is (no chemical feedback) 2.0, 2.9, 1.67, and 1.49–2.67 K (depending on the model assumption), respectively. The same studies suggest a temperature increase of 0.30, 0.26, 0.23, and 0.26–0.44 K, respectively for a doubling of methane and 0.33, 0.65, 0.29, and 0.39–0.66 K for a doubling of nitrous oxide.

The potential impact on the stratosphere of individual gases considered in the present study is now estimated by calculating the steady state ozone and temperature changes for single perturbations, by each of these gases using the fully coupled radiative chemical model. For a doubling of CO_2 a $+1.8\%$ and a $+15\%$ increase are found for the ozone column and for the ozone concentration at 40-km altitude, respectively. The variation in the temperature is -8 K at 40 km. For a doubling of the methane content the corresponding ozone and temperature changes are $+2.35\%$, $+5.5\%$, and $+0.5$ K. A 20% increase, predicted for the concentration of tropospheric ozone, could be considerably higher in regions where large amounts of anthropogenic NO_x are present. If the concentration of N_2O is increased by 20%, the ozone column is reduced by 1.4%, and the ozone concentration at 40 km by 1.8%. A temperature decrease of about 0.3 K is found at 40-km altitude. When the mixing ratio of F-11 and F-12 is uniformly multiplied by 7.5 (leading to a mixing ratio of active chlorine in the upper stratosphere of 9 ppbv), the reduction of the ozone column is 5%, and the decrease of the ozone concentration at 40 km 64.5%. The change in the temperature is -10 K at 40 km. Finally, when all perturbations are considered simultaneously, the ozone depletion (total column) is reduced to 1.1%. The decrease in the concentration of O_3 at 40 km is 51%. The temperature is found to decrease by 25 K at 40-km altitude. These results, which are summarized in Table 4, are in fairly good agreement with other similar studies made, for example, by *Owens et al.* [1985], Wuebbles [see *WMO/NASA*, 1986], and by Bruehl [see *WMO/NASA*, 1986]. These studies predict a change of $+2.9$, $+3.5$ and $+1.2\%$, respectively for a doubling of the CO_2 content, $+4.3$, 2.9, and 1.4% for a doubling in the methane content, and

TABLE 4.　Ozone Changes (Expressed in Percent) for Different Perturbations

Perturbation	Ozone Column	Ozone Concentration at 40 km
$CO_2 \times 2.0$	+1.82	+15.3
$CH_4 \times 2.0$	+2.35	+5.5
$N_2O \times 1.2$	−1.40	−1.8
CFCs $\times$ 7.5	−5.00	−64.5
Combined	−1.11	−50.9

−3.9, −1.7, and −1.2% for a 20% increase in the amount of nitrous oxide.

For continuing emissions of chlorofluorocarbons in the atmosphere equal to 309 kT/yr for F-11 and 433 kT/yr for F-12 the reduction in the ozone column (compared to a preindustrial atmosphere) is estimated to be 5.5% when temperature feedback is omitted in the model calculation and 8.7% when it is included.

3.2. Time-Dependent Calculations

We now deal with the potential changes of the temperature and the ozone concentration in the future based on different scenarios for the release in the atmosphere of the chemical compounds already considered in the previous sections. Future changes in the atmospheric concentration of precursor gases are difficult to predict because of our ignorance in some natural processes involved (for example, our poor understanding of the reasons for methane increases), the uncertain growth in world population, gross national product and energy consumption, unexpected changes in consumer's demand, and uncertainties concerning future regulatory measures for economic growth and environmental protection. *Nordhaus and Yohe* [1983], for example, have considered uncertainties in the future buildup of atmospheric CO_2. From an economic model, in which 10 major variables were randomly modified within a given range of uncertainty, the lowest CO_2 concentration found in year 2100, after 100 model runs, is 370 ppmv, the highest concentration is 2100 ppmv, and the mean con-

centration 780 ppmv. Large uncertainties are also associated with future emissions of other gases such as F-11 and F-12, as shown, for example, by the recent economic study of *Quinn et al.* [1986].

The uncertainties associated with future trends in the emission of precursor gases are probably the largest uncertainties in the prediction of future ozone and temperature variations. Therefore the scenarios used in the present study are not intended to be the most realistic possible but, especially in the case of CO_2, CH_4, and N_2O, are based on extrapolations of past and present growths. For the chlorofluorocarbons, different scenarios will be considered in order to estimate the impact on the ozone abundance of possible regulatory measures dealing with the production of chlorofluorocarbons.

3.2.1.　*Adopted scenarios for the time-dependent model simulations.*　The numerical simulation of the atmospheric behavior is started in year 1910. The results, however, are represented only after 1940 and are expressed relative to the values of this particular year. Through this procedure, the small transient effects appearing during the first steps of integration, as a result of the choice of the initial conditions (which are not necessarily in mutual equilibrium), will not affect the results presented in this paper.

Fifteen scenarios (Table 5) are considered and used in the model calculations to be discussed hereafter. The first four of them (1, 1′, 2, and 2′) assume constant levels of CO_2, CH_4, and N_2O, taken equal to their values in year 1940. Such calculations are not intended to represent a prediction of the future behavior of the atmosphere but are nevertheless performed to isolate the effect of the ClCs. In other words, the numerical results obtained for these conditions should not be associated with the future of the real world.

In the remaining scenarios (3a–8) all greenhouse gases are allowed to vary. The variation as a function of time in the concentration of these gases (except the ClCs) is based essentially on the reference set of scenarios suggested by *Wuebbles et al.* [1984]. For carbon dioxide the historical mixing ratio $X(t)$ is expressed by the analytical expressions (if t is the current year)

$$X(t) = 270 \exp [0.00141(t - 1850)] \text{ ppmv} \qquad (4)$$

TABLE 5.　Scenarios Adopted for the Future

Case	Gases other than ClCs Mixing Ratio	Production of F-11 and F-12			Production of F-113, Rate %/yr	Temperature Feedback
		Rate %/yr	Capacity Cap	Aerosol Ban		
1	constant	3	no	no	not included	yes
1′	constant	3	no	no	not included	no
2	constant	3	yes(1.5)[1]	no	not included	yes
2′	constant	3	yes(1.5)	no	not included	no
3a	increases	0	···	no	not included	yes
3b	increases	0	···	no	3	yes
3c	increases	0	···	no	6	yes
3d	increases	0	···	no	0	yes
4	increases	3	no	yes	6	yes
5a	increases	3	yes(1.5)	no	not included	yes
5b	increases	3	yes(1.5)	no	3	yes
5c	increases	3	yes(1.5)	no	6	yes
6	increases	3	yes(1.5)	yes	6	yes
7	increases	3	yes(2.0)	no	6	yes
8	increases	not included	···	···	not included	yes

CH_3CCl_3 and CCl_4 have constant emission except in scenario 8 where they are not included, and (1.5) means that the capacity cap is 1.5 times the production in 1984.
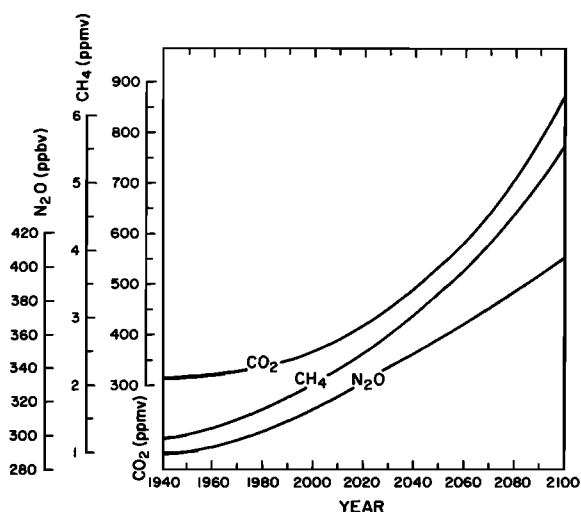
Fig. 8. Variation in the mixing ratio of CO_2, tropospheric CH_4, and tropospheric N_2O as a function of time (1940–2100), adopted in the time-dependent model calculations.

for the period between 1910 and 1957 and

$$X(t) = 270 + 44.4 \exp [0.019(t - 1958)] \text{ ppmv} \quad (5)$$

between 1957 and 1983. After 1983 the following extrapolation is adopted:

$$X(t) = 341.4 + 1.539(t - 1983)$$
$$\cdot \exp [0.009173(t - 1983)] \text{ ppmv} \quad (6)$$

With this projection, based on a study by Edmonds et al. [1984], the CO_2 mixing ratio reaches 600 ppmv in year 2062. In the case of methane, the past mixing ratio is expressed by

$$X(t) = 1.0 + 0.65 \exp [0.035(t - 1980)] \text{ ppmv} \quad (7)$$

for the period 1910–1983. As the cause of the past increase in the methane concentration is not understood and since it is not obvious that the present trend will remain identical in the future, it is difficult to specify for this gas, whose lifetime is of the order of 10 years, a plausible scenario for the next hundred years. Therefore the present growth has been extrapolated after 1983. It should be remembered that this assumption introduces a severe limitation in the ozone and temperature predictions. The historical mixing ratio of nitrous oxide since 1910 is represented by

$$X(t) = 285 + 14 \exp [0.04(t - 1978)] \text{ ppbv} \quad (8)$$

An increase of 0.25%/yr is assumed after 1983. Shown in Figure 8 is the evolution of the mixing ratio of CO_2, CH_4, and N_2O between years 1940 and 2100.

The chlorocarbons CCl_4 and CH_3CCl_3 are assumed to vary with the same rate in all scenarios involved in the present study except scenario 8. The emissions in the atmosphere of carbon tetrachloride (expressed in kilotons per year) are assumed, according to Wuebbles et al. [1984], to be the following between 1910 and 1932:

$$E(t) = 0.96 \exp [0.388(t - 1911)] \quad (1911-1916) \quad (9a)$$

$$E(t) = 6.67 \exp [0.132(t - 1916)] \quad (1916-1922) \quad (9b)$$

$$E(t) = 16.0 \quad (1922-1925) \quad (9c)$$

$$E(t) = 17.1 \exp [0.1067(t - 1925)] \quad (1925-1932) \quad (9d)$$

Between 1932 and 1940 a constant release of 44.1 kT/yr is selected, while for the period 1940–1980 the emissions estimated by Simmonds et al. [1983] are used (lower limit after 1958). For the future a constant emission rate of 100 kT/yr is adopted after 1980. Indeed, better environmental control of the carbon tetrachloride production as an intermediate for the manufacturing of F-11 and F-12 might be expected. Moreover, the use of this product as a grain fumigant is expected to decline and its use as process solvent is small and unlikely to grow to significant levels (CMA, private communication, 1987).

The release in the atmosphere of methyl chloroform was insignificant before 1950. The emission estimated by Prinn et al. [1983] is adopted between 1950 and 1976. Then a linear variation is applied to reach 500 kT in 1980. Future trends in the release of this chemical compound are difficult to estimate. The production of methyl chloroform grew rapidly in the 1970s when it was increasingly used to replace other chlorinated solvents. According to recent economic studies [Conseil Européen des Federations de l'Industrie Chimique, 1985], the market has remained static since 1979 (see also WMO/NASA [1986]). Therefore the release of this gas has been assumed to remain constant for the purpose of the present calculation. This is in contrast to a previous study by Brasseur et al. [1985], in which a substantial increase in the future production of CH_3CCl_3 was assumed. This work, however, indicated that this assumption had only limited effects on the calculated ozone changes.

The emissions of all chlorofluorocarbons used in the model before year 1984 are the same in the first 14 scenarios (1–7). For F-11, emissions of 0.0, 0.1, and 0.2 kT/yr are adopted for the periods 1910–1938, 1938–1943, and 1943–1945, respectively, according to Wuebbles et al. [1984]. Between 1945 and 1984, the emissions derived from the production suggested by the Chemical Manufacturers Association [1985] are used. Emission of F-12 starts in 1931 with a rate of 0.1 kT/yr, reaching 0.4 kT/yr in 1935, and remains constant until 1940 [Wuebbles et al., 1984]. After this period and until 1984 the historical releases derived from CMA production data are adopted. For F-113 the emission starts in 1960 and is based on an estimate of 140 kT/yr in 1984 [WMO/NASA, 1986]. It should be noted that the effect of F-113 is not included in all model cases, as will be explained below.

The emissions of the chlorofluorocarbons introduced in the model for a simulation of the potential atmospheric response after year 1984 may differ greatly from one case to another. They are deduced from the following assumptions on the annual production of these compounds. In cases 3a–3d, the industrial production of F-11 and F-12 is assumed to remain constant and equal to its level of 1984. In cases 1–2' and 4–7, the productions of F-11 and F-12 increase by 3%/yr after 1984 with a delay, however, for cases 4 and 6, resulting from a ban on the use of CFCs as aerosol propellants, assumed to have occurred starting in year 1985. This last assumption is supposed to account for a possible generalization of the regulations taken in the United States and several other countries. Moreover, a production cap equal to 1.5 times the production of 1984 is prescribed in cases 2, 2', 5, 5a, 5b, 5c, and 6. In case 7, the capacity cap is equal to 2 times the 1984 production. The annual growth rate of 3% has been arbitrarily selected but is similar to rates adopted in other studies [WMO/NASA, 1986]. An increase in the release of F-113 is considered in cases 3b, 3c, 4, 5b, 5c, 6, and 7. Use of F-113 is thought to be
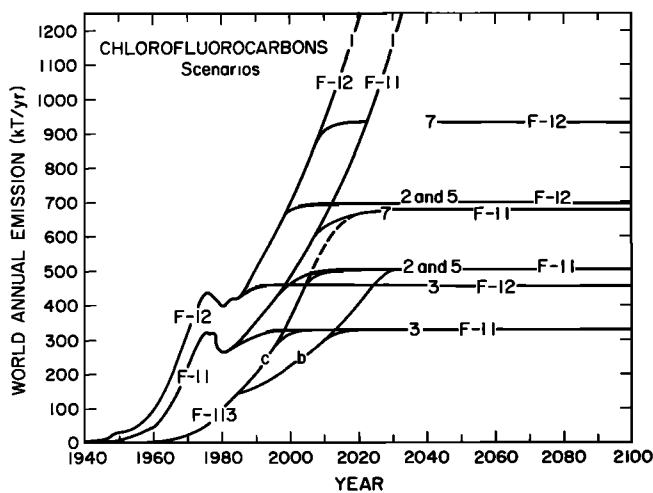
Fig. 9a. Same as Figure 8 but for the world annual emission (kT/yr) of F-11, F-12, and F-113, adopted in different scenarios (1, 2, 3, 5, and 7) listed in Table 5. Note that the emission of F-113 (increase of 3%/yr for case b and 6%/yr for case c) never becomes larger than that of F-11.

TABLE 6a. Past Emission Rates of Chlorocarbons (in Kilotons per Year) as a Function of Time, Adopted in the Model Calculations

| Year | Scenarios 1–7 | | | | Scenarios 3b–4 and 5b–7 |
	CH_3CCl_3	CCl_4	F-11	F-12	F-113
1910	0	0.96	0	0	0
1915	0	6.7	0	0	0
1920	0	12.9	0	0	0
1925	0	19.0	0	0	0
1930	0	32.4	0	0	0
1935	0	44.1	0	0.4	0
1940	0	44.1	0.1	0.4	0
1945	0	69.7	0.2	6.4	0
1950	0	56.0	5.3	25.7	0
1955	8.0	40.7	22.9	47.4	0
1960	36.1	39.7	40.6	91.2	2.5
1965	72.9	72.4	109.2	181.1	6.5
1970	154.5	156.3	209.2	314.7	17.0
1975	364.2	100.1	318.3	435.1	44.3
1980	481.0	97.2	262.6	388.1	97.3

growing fairly quickly at present, as a result of its use in current electronics technology (essentially as a solvent to clean electronic assemblies and components). A growth in the production of 6%/yr is therefore adopted after 1984 in cases 3c, 4, 5c, 6, and 7. However, because there is doubt if this growth rate will be maintained in the longer term, an arbitrary growth rate of 3%/yr has been considered in cases 3b and 5b. In all cases, the emission of F-113 (expressed in mass) is never allowed to exceed that of F-11. A constant F-113 production at the 1984 level is assumed in case 3d. Cases 1–3a and 5a do not include F-113. Figures 9a and 9b show the different emission rates adopted for the chlorofluorocarbons after 1940. Numerical values associated with these curves are given in Tables 6a–6d.

In most cases, the temperature feedback is included in the model calculations. However, in order to assess the importance of the temperature coupling on the ozone response, the "ClC alone" scenarios have been run assuming either fixed temperature during the model integration (cases 1' and 2') or

full radiative coupling including temperature feedback (cases 1 and 2).

3.2.2. Atmospheric response. The ozone and temperature changes calculated in response to the scenarios presented earlier will now be discussed. But in order to be able to compare the quantitative effects of the chlorocarbons to other potential perturbations, a model run (scenario 8), in which no ClC (except CH_3Cl) is included but CO_2, CH_4, and N_2O are increasing, is first presented. Figure 10 shows the change in total ozone and in the ozone concentration at 1 and 50 km, predicted for this particular case. The calculated change in the ozone column is +0.88% in 1985, +1.2% in 2000, +1.7% in 2020, +2.3% in 2040, +3.1% in 2060, +4.1% in 2080 and +5.1% in 2100. This increase results from an enhancement in tropospheric ozone (7.3% in 1985, 9.4% in 2000, 14.6% in 2000, 14.6% in 2040, 21.5% in 2100 at 1 km) and a decrease in stratospheric ozone (−1.6% in 1985, −2.5% in 2000, −4.1% in 2040, −7.0% in 2100). The increase in tropospheric ozone is actually a result of the growth in methane, while the decline in stratospheric ozone is linked essentially to the increase in
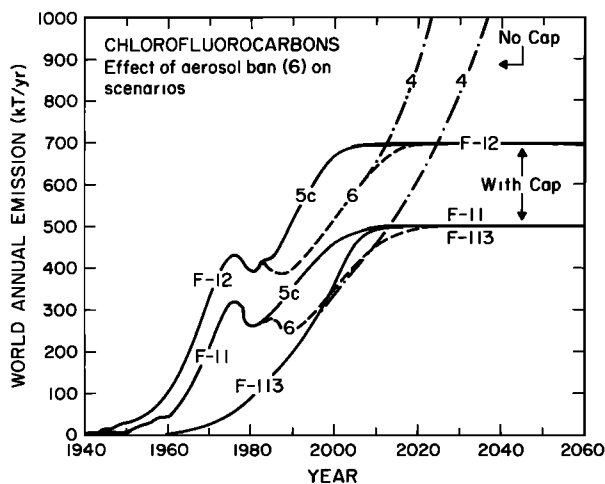

Fig. 9b. Same as Figure 9a but for scenarios 4 and 6 (aerosol ban) compared to case 5c.

TABLE 6b. Future Emissions of F-11 (in Kilotons per Year) Adopted for the Different Scenarios

| Year | Scenarios | | | | | |
	1, 1'	2, 2', 5	3	4	6	7
1985	294.0	294.0	290.5	279.5	279.5	294.0
1990	350.1	350.1	308.3	253.5	253.5	350.1
1995	414.0	414.0	321.6	298.0	298.0	414.0
2000	471.1	471.1	331.2	347.7	347.7	471.1
2010	634.3	497.6	332.9	455.8	455.8	634.3
2020	856.3	503.6	332.9	615.3	494.9	668.7
2030	1156.0	503.6	332.9	830.5	505.5	676.8
2040	1560.6	503.6	332.9	1121.1	505.5	676.8
2050	2106.8	503.6	332.9	1513.3	505.5	676.8
2060	2844.2	503.6	332.9	2042.8	505.5	676.8
2070	3839.7	503.6	332.9	2757.4	505.5	676.8
2080	5183.5	503.6	332.9	3722.1	505.5	676.8
2090	6997.8	503.6	332.9	5024.4	505.5	676.8
2100	9447.1	503.6	332.9	6782.2	505.5	676.8

TABLE 6c. Future Emissions of F-12 (in Kilotons per Year) Adopted for the Different Scenarios

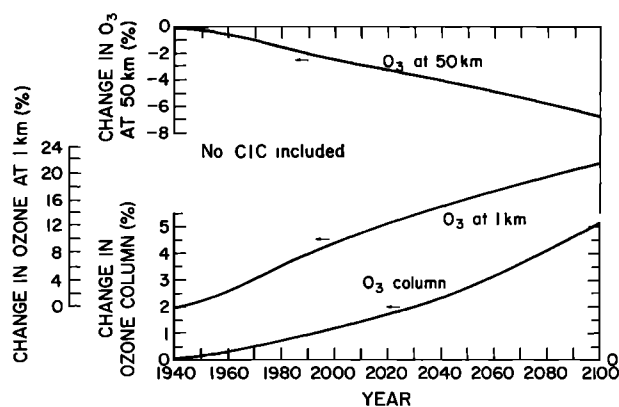| Year	Scenarios					
	1, 1'	2, 2', 5	3	4	6	7
1985	424.1	424.1	420.4	397.0	397.0	424.1
1990	515.3	515.3	457.0	396.2	396.2	515.3
1995	596.8	596.8	457.4	450.6	450.6	596.8
2000	692.5	676.1	458.2	514.8	514.8	692.5
2010	908.6	693.1	458.2	665.7	665.7	908.6
2020	1226.6	693.1	458.2	898.6	688.6	931.5
2030	1655.9	693.1	458.2	1213.0	688.6	931.5
2040	2235.5	693.1	458.2	1637.4	688.6	931.5
2050	3017.9	693.1	458.2	2210.2	688.6	931.5
2060	4074.2	693.1	458.2	2893.5	688.6	931.5
2070	5500.1	693.1	458.2	4027.3	688.6	931.5
2080	7425.2	693.1	458.2	5436.2	688.6	931.5
2090	10024.0	693.1	458.2	7338.1	688.6	931.5
2100	13532.4	693.1	458.2	9905.4	688.6	931.5

Fig. 10. Relative variation in the ozone column and in the ozone concentration at 1- and 50-km altitude, calculated as a function of time (1940–2100) for perturbations in CO_2, CH_4, and N_2O, as specified in Figure 8. The impact of man-made chlorocarbons is ignored in this calculation.

nitrous oxide. In this calculation the mixing ratio of NO_x is of the order of 50 pptv in the middle troposphere. It should be noted that since the effect of thermal inertia provided by the global ocean is neglected in the model, the calculated time history of tropospheric ozone shown in Figure 10 (and in Figure 17) might be somewhat approximate, since the surface temperature influences tropospheric water vapor, tropospheric OH, and hence the global tropospheric chemistry. The primary effects influencing future tropospheric ozone changes appear, however, to be rapid growths in methane and nitrogen oxides.

To determine how rapidly the stratospheric ozone responds to the release in the atmosphere of the ClCs, it should be remembered that the global lifetime of molecules such as F-11 and F-12 is significantly longer than the photochemical lifetime of these molecules in the upper stratosphere where their destruction takes place (~ 1 year at 30 km) and than the characteristic time associated with vertical transport of these species from their source to their sink region. As shown by Stordal et al. [1985], the long turnover time for source gases, which are essentially inert in the lower atmosphere, is explained by the large differences in density between the level where they are emitted (surface) and where they are destroyed (30–40 km). When free chlorine atoms are released in the

upper stratosphere, essentially by photodecomposition of the ClCs, they react rapidly with ozone, whose chemical lifetime at these heights is of the order of a day. In order to estimate the response time of the atmosphere to ClC perturbations, a time-dependent model run has been performed (with constant amounts of CO_2, CH_4, and N_2O). In this run the emission of the ClCs (except CH_3Cl) has been arbitrarily put to zero after 1984. The behavior of Cl_x and of the ozone column before and after this total ClCs ban is shown in Figure 11. It can be seen that the mixing ratio of Cl_x at 50 km continues to increase during approximately 16 years and then recovers very slowly. The ozone column continues to decrease during 8 years (and not 16 years, as Cl_x below 50 km recovers sooner than at the stratopause). After 1993 the column builds up and reaches the 1985 value in year 2025 and the 1976 value in year 2080.

Attention will now be given to the "ClC alone" cases in order to understand the specific long-term effects of these compounds. Again, these scenarios are not intended to simulate the real world, as the growth in the chlorocarbons will manifest itself together with the increase of the other trace gases. Shown in Figure 12 is the change in the ozone column derived for the two scenarios assuming a fixed temperature (cases 1' and 2') or allowing the temperature to vary (cases 1 and 2). For both scenarios the response including temperature
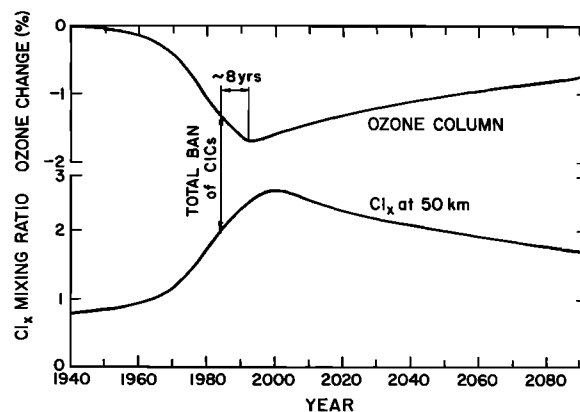
TABLE 6d. Future Emissions of F-113 (in Kilotons per Year) Adopted for the Different Scenarios

Year	Scenarios							
	3b	3c	3d	4	5b	5c	6	7
1985	144.2	148.4	140.0	148.4	144.2	148.4	148.4	148.4
1990	167.1	198.6	140.0	198.6	167.1	198.6	198.6	198.6
1995	193.8	265.7	140.0	265.7	193.8	265.7	265.7	265.7
2000	224.6	331.2	140.0	347.7	224.6	355.6	347.7	355.6
2010	301.9	332.9	140.0	455.8	301.9	497.6	455.8	561.0
2020	332.9	332.9	140.0	615.3	405.7	503.6	494.9	632.6
2030	332.9	332.9	140.0	830.5	503.6	503.6	505.5	676.8
2040	332.9	332.9	140.0	1121.1	503.6	503.6	505.5	676.8
2050	332.9	332.9	140.0	1513.3	503.6	503.6	505.5	676.8
2060	332.9	332.9	140.0	2042.8	503.6	503.6	505.5	676.8
2070	332.9	332.9	140.0	2757.4	503.6	503.6	505.5	676.8
2080	332.9	332.9	140.0	3722.1	503.6	503.6	505.5	676.8
2090	332.9	332.9	140.0	5024.4	503.6	503.6	505.5	676.8
2100	332.9	332.9	140.0	6782.2	503.6	503.6	505.5	676.8

Fig. 11. Evolution of the Cl_x mixing ratio at 50-km altitude and of the change in the ozone column if the emission of ClCs are totally stopped in year 1985.
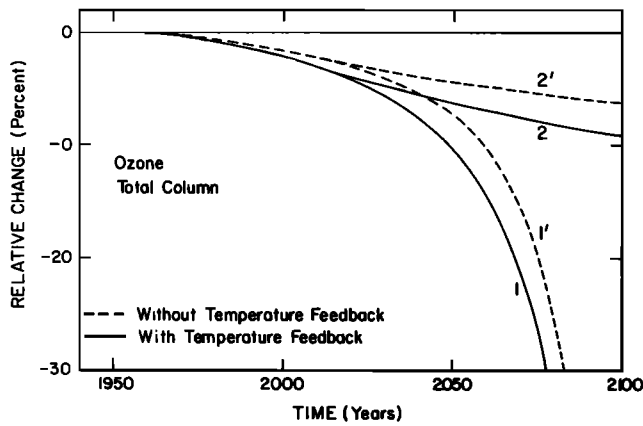
Fig. 12. Relative change in the ozone column for cases 1 and 1' (increase of 3%/yr in the F-11 and F-12 production rate) and for cases 2 and 2' (production of F-11 and F-12 assumed to remain constant at their 1985 level). The effect of a CO_2, CH_4, and N_2O increase is not taken into account. Calculations with and without temperature feedback are shown.

feedback is larger than if the temperature is not allowed to change. This is fully consistent with the results discussed earlier when steady state conditions were assumed. If no limitation is imposed on global CFC production (cases 1 and 1'), the ozone depletion becomes dramatic especially after year 2040 as it reaches values larger than 20% in 2070 and larger than 30% 8–10 years later. The mixing ratio of total inorganic chlorine in the upper stratosphere reaches 2.8 ppbv in year 2000, 5.2 in 2020, 9.3 in 2040, 16.0 in 2060, and 29.0 in 2080. These latter values are so high that essentially all NO_x molecules are titrated by Cl_x, so that a strong nonlinear behavior is predicted by the model. When a capacity cap of 1.5 times the present CFC production level is applied (cases 2 and 2'), the reduction in the ozone column is significantly reduced (2.5% in 2000, 5.5% in 2040, and 9% in 2100, when the temperature feedback is included). The change appears to be essentially
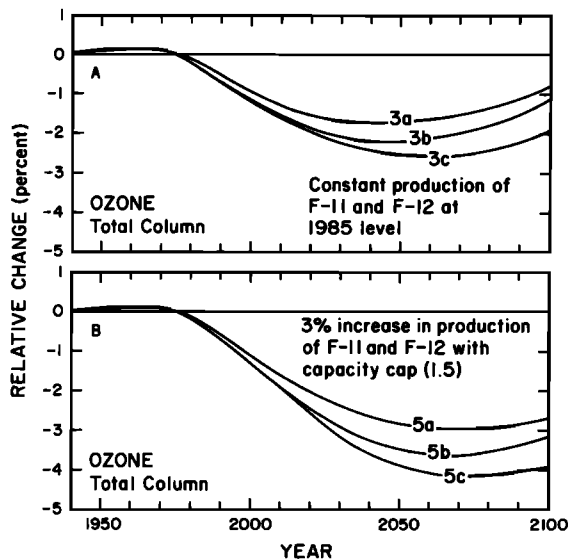

Fig. 13. Relative change in the ozone column for (a) cases 3a–3c and (b) cases 5a–5c between 1940 and 2100. The effect of a simultaneous increase in CO_2, CH_4, and N_2O (Figure 8) is taken into account.
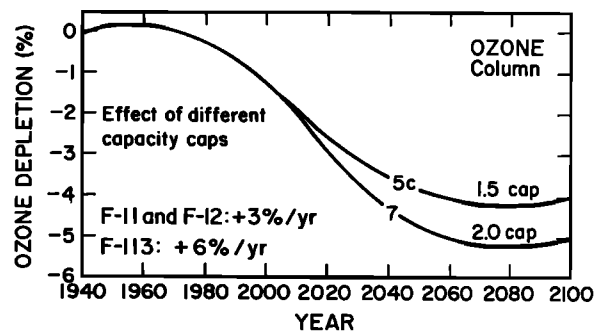

Fig. 14. Effect of different capacity caps (1.5 and 2.0 times the present production level of F-11 and F-12) on the change in the ozone column between years 1940 and 2100.

linear with time. Indeed, the relative concentration of total chlorine is 2.7 ppbv in year 2000, 4.8 in 2020, 6.8 in 2040, 8.5 in 2060, 10.0 in 2080, and 11.3 in 2100 and thus never exceeds the mixing ratio of total NO_x.

We now consider somewhat the more realistic cases (3–7) in which all perturbations are involved simultaneously. In these model simulations the effect of the temperature feedback is fully included. However, the change in the chemical composition associated with the variation in the solar ultraviolet irradiance over an 11-year solar cycle is not considered. But from the model calculations of Brasseur et al. [1987] and the analysis of satellite data by Keating et al. [1987] it can be deduced that between solar maximum and solar minimum the ozone column should be reduced by 1.7 ± 1% and the ozone concentration in the upper stratosphere (2 mbar) by 2 ± 1%. These periodic variations have to be superimposed on the long-term changes associated with the anthropogenic perturbations.

The change in the ozone column for a constant F-11 and F-12 production at the 1984 level, including the effect of the expected CO_2, CH_4, and N_2O increase, is shown in Figure 13a. The different curves correspond to different conditions for the F-113 emission. In all cases, the ozone content increases slightly between 1940 and 1970, as, during this period, the effects of carbon dioxide and methane largely compensate the action of the ClCs and of nitrous oxide. The increase, however, is never larger than 0.1% and is thus too small to have been detected. After 1970 the ozone starts to be depleted essentially by anthropogenic chlorine. The rate of decrease is, for example, larger in case 3c than 3a, showing the long-term effect of F-113. After year 2040 in case 3a and 2060 in case 3c the ozone column starts to increase again as a result of the fast growth in methane. This effect will be discussed in more detail when the altitude dependence of the ozone response will be considered. Similar cases, but for a 3%/yr increase in the F-11 and F-12 production, with a capacity cap of 1.5 times the 1984 production level, are shown in Figure 13b. As in the previous cases, after a small increase before 1970 the ozone column starts to decrease to reach for case 5a a maximum reduction of 2.8% in 2070 and for case 5c a maximum reduction of 4.2% in 2080. Thereafter, a slow increase takes place.

Different measures have been suggested to regulate the production or the use of the chlorofluorocarbons. We now consider the impact of two possible regulatory measures: (1) the adoption of a cap below which the world production capacity of the CFCs must remain; the sensitivity of the ozone column
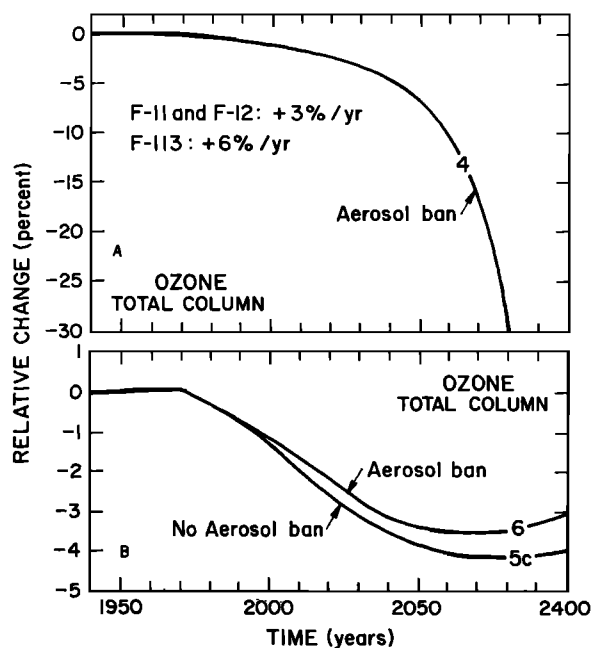
Fig. 15. Effect of a ban in the use of F-11 and F-12 as aerosol can propellants on the change in the ozone column (*a*) without capacity cap (case 4) and (*b*) with capacity cap (case 6 compared to case 5c).
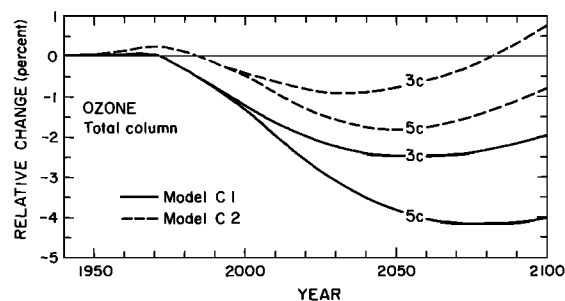

Fig. 16. Comparison between changes in the ozone column for scenarios 3c (constant production in CFCs at the 1985 level) and 5c (3% increase in the CFCs production with a capacity cap at 1.5 times the 1985 level), obtained with radiative codes C1 and C2, respectively.

to the level of this cap will be considered and (2) an immediate total ban of the CFCs as propellant agents in aerosol cans. For brevity this latter case will be referred as "aerosol ban."

The ozone response, calculated for two different levels of the capacity cap (1.5 times the 1984 production (case 5c) and 2.0 times this level (case 7)) is shown in Figure 14. In both cases, the increase of the F-11 and F-12 production, after 1984 and before the capacity cap is reached, is assumed to be 3%/yr. The emission rate of F-113 increases by 6%/yr until it reaches the emission level of F-11 and remains constant thereafter. In both cases, the ozone depletion is significantly lower than when no cap is applied. Furthermore, the maximum ozone depletion, which is 4.2% when a capacity cap of 1.5 is adopted, becomes 5.2% when this cap equals 2 times the 1984 production level.

If the future 3% increase in F-11 and F-12 is delayed by an aerosol ban and if no capacity cap is applied, the ozone depletion is also delayed but finally reaches dramatic levels. Figure 15*a* indicates that in a case similar to 5c but with an aerosol ban and no capacity cap (case 4) the ozone reduction (referred to the 1940 value) is less than 1% before 1990 and less than 2% before 2015 but reaches 10% in 2060 and 30% in 2080. Finally, the case referring to an aerosol ban with capacity cap (case 6) is compared in Figure 15*b* to a similar case (5c) with the same capacity cap but no aerosol ban. It clearly appears that the difference between the two model predictions is small (less than 0.5%) until 2055. In 2100 the difference is less than 1%.

In order to estimate the possible model dependence of these results, model simulations with scenarios 3c and 5c have also been performed with the radiative code C2. Again, it should be remembered that this code is conceptually different from code C1, although both of them provide results for the present-day atmosphere which are in fairly good agreement with the observation. The calculated change in the ozone

column for the two models and the two perturbation cases is shown in Figure 16. Obviously, model C1 (which is used in most of this paper) leads to larger ozone reductions. For example, in case 5c, the maximum ozone reduction is 4.2% when model C1 is used and 1.8% only with model C2. This has, at least in part, to be attributed to the difference in the temperature change calculated by the two models in the region where most of the ozone is confined and where, despite the fact that the chemical lifetime of ozone becomes larger than the dynamical lifetime, the sensitivity of the ozone chemistry to the temperature changes is still significant. Such a comparison of two models, in which the chemistry is entirely identical, clearly shows that differences in the results obtained by the several models used, for example, in the *WMO/NASA* [1986] intercomparison are not surprising.

The change in the ozone column, which has been previously discussed, is an important parameter to assess the expected variation in the ultraviolet irradiance at the earth's surface and the related biological consequences. The determination of the changes in local ozone is also important since the heating rate and, consequently, the temperature depend not only on the transmission of solar UV radiation in the atmosphere but also on the ozone concentration as a function of altitude. Changes in ozone, especially in the stratosphere, and related variations in the temperature may cause significant modifications in the general circulation of the atmosphere with potential effects in the troposphere. These dynamical feedbacks, as well as their impacts on the earth's climate, are difficult to assess quantitatively. As they require sophisticated three-dimensional models, they will not be considered in the present study.

The effect, as a function of height, of increasing emissions of trace gases will be discussed for one particular case, namely scenario 5c. Figure 17*a* shows the change in the ozone concentration as a function of height for years 2000, 2040, and 2100, and Figure 17*b* the same variations but expressed as a function of time, at selected altitudes from the surface to 50 km. Clearly, ozone is significantly depleted above 25 km with a maximum (for the relative change) at 40 km. The rate of change is rapid after 1990 but decreases after 2020 and tends even to zero around 2100. In fact, during the last part of the integration the amount of methane is so high that most chlorine atoms are rapidly converted into HCl. In the lower stratosphere and in the troposphere, ozone increases as a function of time. This behavior results from the self-healing effect of the atmosphere but also, particularly in the troposphere, from the enhanced methane concentration. Indeed, methane in
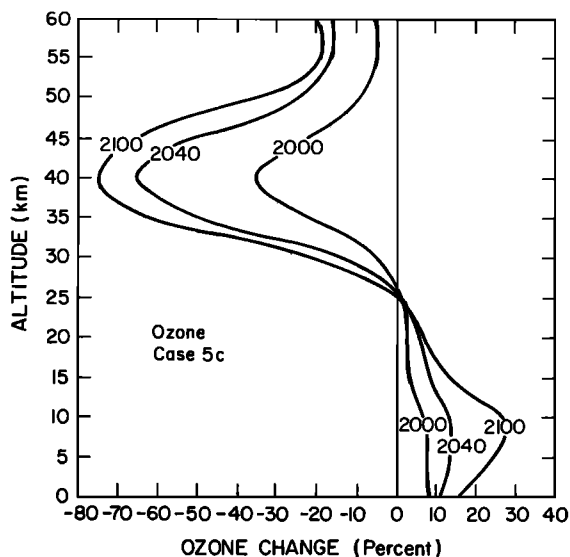
Fig. 17a. Relative variation (percent) of the ozone concentration between 0- and 60-km altitude calculated for years 2000, 2040, and 2100, in the case of scenario 5c (3%/yr increase in F-11 and F-12 with capacity cap at 1.5 times the 1985 production level, 6%/yr increase in F-113 emission with an upper limit equal to the emission of F-11, increase in the concentration of other trace gases (see Figure 8), temperature feedback included).

the presence of nitrogen oxides may produce significant amount of ozone below 15-km altitude. According to the model, the increase in the tropospheric O_3 concentration in 1985 compared to 1940 should be of the order of 5%. It could reach, on the average, 25–30% in year 2100.

The change in the temperature profile is shown in Figure 18 as a function of time for 20-, 30-, 40-, and 50-km altitude. A cooling is predicted above 30 km with a maximum at 45 km. These temperature changes, resulting from the decrease in the ozone concentration and the increase in the amount of carbon dioxide, are sufficiently large to induce significant dynamical perturbations.

4. UNCERTAINTIES IN MODEL CALCULATIONS

The results given previously to characterize the chemical and radiative response of the atmosphere, especially the vari-
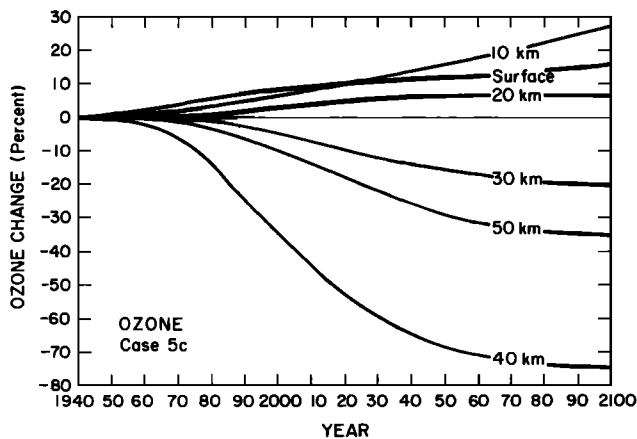

Fig. 17b. Relative variation (percent) as a function of time (1940–2100) of the ozone concentration calculated at selected altitudes for scenario 5c (same conditions as in Figure 17a).
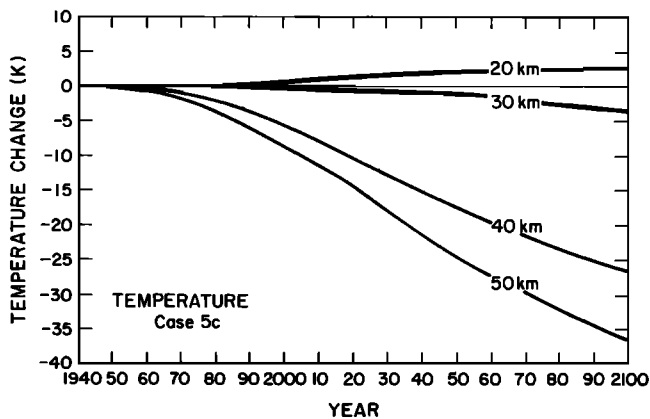

Fig. 18. Same as Figure 17b but for the variation (Kelvin) in temperature.

ation in the total ozone content, are somewhat uncertain. Indeed, the reduction in the ozone column, which is of the order of a few percent, is a difference between two large variations in the O_3 concentration: The first of them, located in the upper stratosphere, results from direct chemical actions including significant temperature feedback effects and the second, occurring at lower altitude in the region where most of the ozone is confined, is largely a consequence of the self-healing effect. In other words, the resulting column change is highly dependent on the treatment of the nonlinear transmission of solar radiation in the atmosphere. Moreover, as shown by a comparison of the results provided by the two radiative
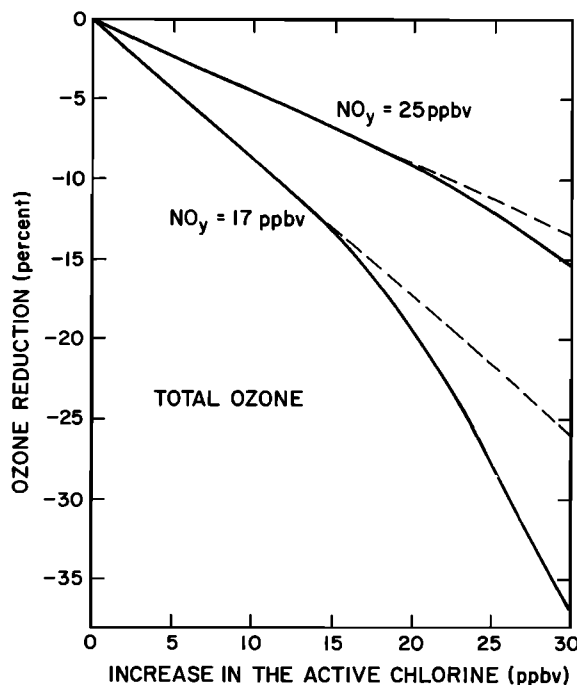

Fig. 19. Relative change in the ozone column as a function of additional amounts of active chlorine in the atmosphere for two different levels of odd nitrogen. The vertical profiles of Cl_x and NO_y assumed for this calculation are similar in shape to those shown in Figure 7. The values appearing on this graph refer to the mixing ratio of Cl_x at 50 km and of NO_y at 35 km.

codes involved in the present study, the calculated temperature change in the middle and lower stratosphere impacts significantly on the calculated change in the ozone column. It is thus important for one-dimensional models to treat with some detail the radiative transfer processes, including convective adjustment, all the way down to the surface, instead of using simpler codes in which radiative equilibrium conditions are assumed.

Uncertainties also remain in the chemical scheme which is adopted. For example, one-dimensional models usually predict a maximum mixing ratio of 13–20 ppbv [*WMO/NASA*, 1986] for total active nitrogen (NO_y) near 35 km, while values inferred from LIMS data [*Gille et al.*, 1984; *Russell et al.*, 1984; *Callis et al.*, 1985] suggest maximum values larger than 20 ppbv and probably close to 24 ppbv. As seen in Figure 19, the background amount of NO_y is a crucial parameter for the calculation of the ozone depletion by active chlorine (see also *Brasseur et al.* [1985] and *Isaksen and Stordal* [1986]). Indeed, the sensitivity of ozone to chlorine is reduced by approximately a factor of 2 when the NO_y mixing ratio is increased from 17 to 25 ppbv. Moreover, the range over which the ozone response is linear with the buildup of Cl_x becomes wider when the amount of odd nitrogen increases. For an enhancement in the Cl_x mixing ratio ΔCl_x (at 50 km) of less than 15 ppbv (linear regime) and for an NO_y relative concentration (at 35 km) between 17 and 25 ppbv the variation in the ozone column (ΔO_3) can be expressed by the following numerical expression:

$$\Delta O_3(\%) = \{-1.725 + 0.05[NO_y]\}\Delta Cl_x \qquad (10)$$

where $[NO_y]$ and ΔCl_x are expressed in ppbv. This expression was obtained from an interpolation of the model results for which the amount of other species such as CH_4, N_2O, and CO_2 was kept fixed. Parametric expressions for various conditions, including simultaneous increases in the atmosphere content of different gases are given by P. S. Connell (preprint, 1986). As our model calculations probably underestimate the amount of active nitrogen in the atmosphere, the calculated ozone depletions related to increasing emissions of ClCs might represent upper limits. Further consideration should be given to the nitrogen budget in the stratosphere in order to resolve the discrepancy between observed and calculated amounts of NO_y.

Uncertainties in the chlorine chemistry are still important. For example, as noted by *Brasseur et al.* [1985] and more recently by *Isaksen and Stordal* [1986], the calculated ozone depletion is sensitive to the relative efficiency of both channels in reactions

$$ClO + OH \rightarrow Cl + HO_2 \qquad (11a)$$

$$ClO + OH \rightarrow HCl + O_2 \qquad (11b)$$
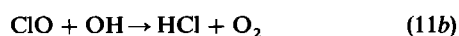
The reaction scheme recommended by *DeMore et al.* [1985] does not consider path (11b) but, if a probability of occurrence of 15% is assumed according to *Burrows et al.* [1984], the calculated ozone depletion should be reduced by 25–30%. Additional laboratory work on this problem is urgently required.

Finally, the calculated ozone depletion is significantly affected by the value of the eddy diffusion coefficient which is adopted. The steady state ozone variation resulting from identical CFC emissions, calculated with the same model input, except for the eddy diffusion coefficient (see Figure 2), is
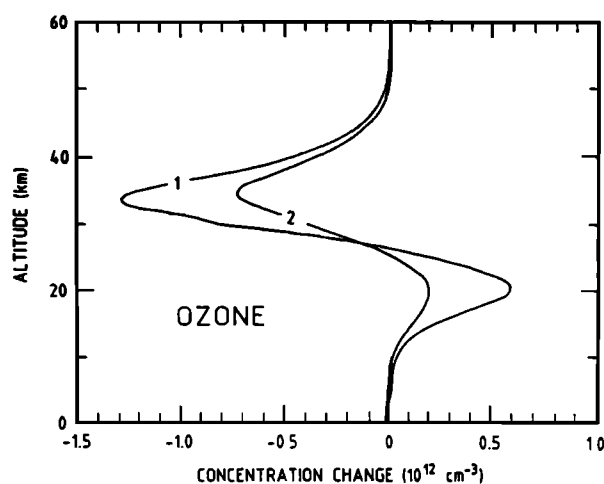

Fig. 20. Effect of different eddy diffusion profiles (see Figure 2 for the definition of cases 1 and 2) on the ozone change in response to a CFC perturbation.

shown in Figure 20. As the vertical transport and lifetime of the source gas are greatly affected by the strength of the average vertical exchanges in the atmosphere, the vertical distribution of these source gases and, consequently, of the active species is modified together with the K coefficient. The model shows, for example, that the maximum value of the NO_x mixing ratio is increased when vertical exchanges are stronger. This situation arises because the N_2O concentration in the upper stratosphere is enhanced. In contrast, the concentration of active chlorine (Cl, ClO) in the upper stratosphere and, consequently, the loss rate of ozone by odd chlorine is reduced as the eddy diffusion coefficient becomes larger. This is a direct consequence of the stronger upward transport of methane which converts active chlorine into HCl.

Thus stronger vertical exchanges (large eddy diffusion coefficients) enhance the contribution of NO_x and simultaneously reduce that of Cl_x to the total ozone loss rate. In other words, the sensitivity of ozone to the CFCs decreases as the adopted eddy diffusion coefficient increases. For example, if the depletion of the ozone column for a CFC perturbation is estimated to be 7.9% for the nominal K profile (labeled 1 in Figure 2) used in this work, it is reduced to 5.9% when the larger eddy diffusion coefficient (labeled 2 in Figure 2) is adopted. Also, the nonlinear regime of the O_3/Cl_x effect is reached sooner for the slower vertical exchanges as, in this case, the value of the Cl_x mixing ratio reaches that of NO_x more rapidly.

Another limitation in the accuracy of the model arises from its dimensionality. Multidimensional approaches clearly tend to represent more realistically the behavior of the atmosphere. Serious problems, however, remain in the representation by these models of the zonally averaged circulation and, consequently, of the meridional transport of trace gases such as NO_y or Cl_x.

Two-dimensional studies assuming fast horizontal diffusion (e.g., *Brasseur and Bertin* [1978] and U. Schmailzl, as quoted by *WMO/NASA* [1986]) indicate very little latitudinal and seasonal variability of the ozone response to increasing trace gases concentration. In contrast, other models with slower eddy diffusion [e.g., *Haigh and Pyle*, 1982; *Solomon et al.*, 1985; *Stordal and Isaksen*, 1987] suggest that transport effects will likely lead to latitudinal and seasonal variations in the ozone response. Meridional transport by planetary wave tran-

sience and dissipation remains difficult to treat accurately in two-dimensional models, especially for periods during which large dynamical disturbances are observed. As noted recently by *Kouker and Brasseur* [1986], during such events, transport becomes particularly strong, and two-dimensional models are no longer appropriate to simulate the transport of trace species in the stratosphere, especially at high latitude.

5. SUMMARY

Calculations using an interactive chemical-radiative-transport one-dimensional model show that increasing concentrations in the atmosphere of source gases such as CO_2, CH_4, N_2O, and the chlorocarbons should significantly modify the ozone and temperature distributions in the stratosphere and the troposphere.

1. Calculations based on time-dependent scenarios and assuming a 3%/yr growth for the F-11 and F-12 production with a capacity cap of 1.5 times the 1984 production level indicate that the reduction in the ozone column in the period 1940–2100 is less than 10%, assuming that the concentrations of these latter gases are increasing according to the scenarios adopted in this study, the maximum ozone depletion is 2.8% and occurs in year 2060. The slow recovery predicted afterward results essentially from increasing concentrations of ozone in the troposphere (due to enhanced CH_4 amounts). If, in addition, a 6% increase is assumed for F-113 (with an emission rate expressed in mass units which never exceeds that of F-11), the maximum ozone depletion (appearing in year 2070) is 4.2%. If a capacity cap of 2.0 times the 1984 production level is adopted for F-11 and F-12, instead of 1.5, the ozone reduction is enhanced by about 1% in the second half of the twenty-first century. Finally, if no capacity cap is applied, the ozone depletion calculated for a 3%/yr growth rate in the production of F-11, and F-12 becomes significantly larger than 10% after year 2050, even if a ban is imposed for the use of CFCs as propellant agents in aerosol cans. In this case, the ozone response is delayed by a few years.

2. Even if the changes in the ozone column remain limited, large variations in the local concentration of O_3 appear in certain altitude ranges. For example, in the upper stratosphere near 40 km, reductions of 60–70% in the ozone concentration are predicted. These large numbers have a small influence on the ozone column since (1) at these heights, the ozone density represents less than 10% of the density near 20–25 km and (2) the reduction in the upper stratosphere is partly balanced by an ozone increase at lower levels. However, these large local changes have potential effects on dynamical parameters. These effects need to be investigated by multidimensional models such as general circulation models.

3. Despite numerous improvements in our understanding of atmospheric chemistry in the last decade or so, large uncertainties (a factor of 2–3) are associated with calculated variations in the ozone column. The largest errors are undoubtedly due to uncertainties in future emission rates, which have to be obtained from economic analyses. Errors in the calculation of the atmospheric response to specific perturbations arise not only because of uncertainties in measured rate constants or absorption cross sections, or eventual missing chemistry in the model, but also because of a lack of knowledge in the budget of active nitrogen, of approximations made in the treatment of radiative transfer, and of simplified treatment of atmospheric transport. In fact, two-dimensional models [*Isak-*

sen and Stordal, 1986] should provide some insight as to the latitudinal and seasonal dependences of the ozone and temperature response to man-made perturbations.

4. The calculated ozone and temperature changes calculated by the model are believed to represent upper limits (assuming that no major reaction is missing in the chemical scheme) since (1) the amount of odd nitrogen (17–18 ppbv at 35 km) derived by the model (and by most other models) appears to be lower than the value inferred from the observation of NO, NO_2, and HNO_3, (2) the ozone depletion obtained when using radiative code C1 (as in most simulations presented in this paper) are significantly higher than when code C2 is used, (3) the change in the ozone column predicted, as in most of this study, with weak vertical exchanges (profile 1 of the eddy diffusion coefficient; see Figure 2) is larger than when eddy diffusion is assumed to be faster (profile 2), (4) the effect of the oceans which delays the temperature response of the atmosphere is not included, and (5) the sources of active nitrogen in the troposphere remain constant, despite the fact that the strength of the NO_x pollution (combustion processes) is expected to grow in the future.

In conclusion, the ozone concentration and the temperature are expected to decrease in the upper stratosphere, as a result essentially of emissions of chlorofluorocarbons in the atmosphere. The ozone content is expected to increase in the troposphere, as a consequence of increasing concentrations of methane and nitrogen oxides. Due to enhanced greenhouse effects the earth's surface should warm up by several degrees. The amplitude and even the sign of future changes in the ozone column are difficult to predict, as they are strongly scenario-dependent (see also *De Rudder and Brasseur* [1985]). An early detection system to prevent noticeable ozone changes as a result of increasing concentrations of source gases should thus be based on a continuous monitoring of the ozone amount in the upper stratosphere rather than on measurements of the ozone column only. Measurements of NO_x, Cl_x, and HO_x will also be required for unambiguous trend detection and interpretation.

REFERENCES

Ackerman, M., D. Frimout, C. Muller, and D. J. Wuebbles, Stratospheric methane measurements and predictions, *Pure Appl. Geophys., 117,* 367–380, 1978.

Blake, D. R., W. E. Mayer, S. C. Tyler, Y. Makide, D. C. Montague, and F. S. Rowland, Global increase in atmospheric methane concentrations between 1978 and 1980, *Geophys. Res. Lett., 9,* 477–480, 1982.

Brasseur, G., Ozone and temperature trends due to the injection of trace species in the atmosphere, in *Stratosphere, Proceedings of a Working Party Meeting,* 95 pp., Commission of the European Communities, Brussels, Belgium, 1984.

Brasseur, G., and M. Bertin, The action of chlorine on the ozone layer

as given by a zonally averaged two-dimensional model, *Pure Appl. Geophys.*, *117*, 436–450, 1978.

Brasseur, G., and P. C. Simon, Stratospheric chemical and thermal response to long-term variability in solar UV irradiance, *J. Geophys. Res.*, *86*, 7343–7362, 1981.

Brasseur, G., A. De Rudder, and C. Tricot, Stratospheric response to chemical perturbations, *J. Atmos. Chem.*, *3*, 261–288, 1985.

Brasseur, G., A. De Rudder, G. M. Keating, and M. C. Pitts, Response of middle atmosphere to short-term solar ultraviolet variations, 2, Theory, *J. Geophys. Res.*, *92*, 903–914, 1987.

Bruehl, C., An efficient model for changes of global climate and composition of the atmosphere due to human activities, Ph.D. thesis, Univ. of Mainz, Mainz, Federal Republic of Germany, 1986.

Bruehl, C. H., and P. J. Crutzen, A radiative-convective model to study the sensitivity of climate and chemical composition of a variety of human activities, in *Stratosphere, Proceedings of a Working Party Meeting*, pp. 85–94, Commission of the European Communities, Brussels, Belgium, 1984.

Burrows, J. P., T. J. Wallington, and R. P. Wayne, Kinetics of the reaction of OH with ClO, *J. Chem. Soc. Faraday Trans.*, *80*, 957–971, 1984.

Callis, L. B., M. Natarajan, and R. E. Bougher, On the relationship between the greenhouse effect, atmospheric photochemistry, and species distributions, *J. Geophys. Res.*, *88*, 1401–1426, 1983.

Callis, L. B., M. Natarajan, and J. M. Russell, III, Estimates of the stratospheric distributions of odd nitrogen from the LIMS data, *Geophys. Res. Lett.*, *12*, 259–262, 1985.

Chemical Manufacturers Association (CMA), Production sales and calculated release of chlorofluorocarbons 11 and 12 through 1984, report, Fluorocarbon Program Panel, Washington, D. C., October 1985.

Cicerone, R. J., D. H. Stedman, and R. S. Stolarski, Estimate of late 1974 stratospheric concentration of gaseous chlorine compounds, *Geophys. Res. Lett.*, *2*, 219–222, 1975.

Connell, P. S., and D. J. Wuebbles, Ozone perturbations in the LLNL one-dimensional model—Calculated effects of projected trends in CFCs, CH_4, CO_2, N_2O and halons over 90 years, report, Univ. of Calif. Radiat. Lab., Livermore, 1986.

Conseil Européen des Federations de l'Industrie Chimique (CEFIC), *Halocarbon Trend Study 1983–1995*, European Council of Manufacturers Federations, Brussels, Belgium, 1985.

Crutzen, P. J., The influence of nitrogen oxides on the atmospheric ozone content, *Q. J. R. Meteorol. Soc.*, *96*, 320–325, 1970.

Crutzen, P. J., Ozone production rates in an oxygen, hydrogen, nitrogen oxide atmosphere, *J. Geophys. Res.*, *76*, 7311–7327, 1971.

Crutzen, P. J., Photochemical reactions initiated by and influencing ozone in unpolluted tropospheric air, *Tellus*, *26*, 47–57, 1974.

Crutzen, P. J., The role of the tropics in atmospheric chemistry, in *Geophysiology of Amazonia*, edited by R. Dickinson, Wiley-Interscience, New York, 1986.

Crutzen, P. J., L. E. Heidt, J. P. Krasnec, W. H. Pollock, and W. Seiler, Biomass burning as a source of atmospheric gases CO, H_2, N_2O, NO, CH_3Cl and COS, *Nature*, *282*, 253–256, 1979.

Cunnold, D., F. Alyea, N. Phillips, and R. Crinn, A three-dimensional dynamical-chemical model for atmospheric ozone, *J. Atmos. Sci.*, *32*, 170–194, 1975.

De More, W. B., D. M. Golden, R. F. Hampson, M. J. Kurylo, C. J. Howard, J. J. Margitan, M. J. Molina, and A. R. Ravishankara, Chemical kinetics and photochemical data for use in stratospheric modeling, *Eval. 7, JPL Publ. 85-37*, Jet Propul. Lab., Pasadena, Calif., 1985.

De Rudder, A., and G. Brasseur, Ozone in the 21st century: Increase or decrease?, in *Atmospheric Ozone, Proceedings of the Quadrennial Ozone Symposium held in Halkidiki, Greece, September 3–7, 1984*, edited by C. S. Zerefos and A. Ghazi, pp. 92–96, D. Reidel, Hingham, Mass., 1985.

Dickinson, R. E., Convergence rate and stability of ocean-atmosphere coupling schemes with a zero-dimensional climate model, *J. Atmos. Sci.*, *38*, 2112–2120, 1981.

Dickinson, R. E., and R. J. Cicerone, Future global warming from atmospheric trace gases, *Nature*, *319*, 109–115, 1986.

Donner, L., and V. Ramanathan, Methane and nitrous oxide: Their effects on the terrestrial climate, *J. Atmos. Sci.*, *37*, 119–124, 1980.

Edmonds, J. A., J. Reilly, J. R. Trabalka, and D. E. Reiche, An analysis of possible future retention of fossil fuel CO_2, the technical report, Carbon Dioxide Res. Div., U.S. Dep. of Energy,

Washington, D. C., 1984.

Fabian, P., Halogenated hydrocarbons in the atmosphere, in *The Handbook of Environmental Chemistry*, vol. 4, pp. 23–51, Springer Verlag, New York, 1986.

Gille, J. C., and L. V. Lyjak, Radiative heating and cooling rates in the middle atmosphere, *J. Atmos. Sci.*, *43*, 2215–2229, 1986.

Gille, J. C., J. M. Russell, III, P. L. Bailey, E. E. Remsberg, L. L. Gordley, W. F. J. Evans, H. Fischer, B. W. Gandrud, A. Girard, J. E. Harries, and S. A. Beck, Accuracy and precision of the nitric acid concentrations determined by the limb infrared monitor of the stratosphere experiment on Nimbus 7, *J. Geophys. Res.*, *89*, 5179–5190, 1984.

Graedel, T. E., The kinetic photochemistry of the marine atmosphere, *J. Geophys. Res.*, *84*, 273–286, 1979.

Haigh, J. D., and J. Pyle, Ozone perturbations in a two-dimensional circulation model, *Q. J. R. Meteorol. Soc.*, *108*, 551–574, 1982.

Harper, D. B., Halomethane from halide ion—A highly efficient fungal conversion of environmental significance, *Nature*, *315*, 55–57, 1985.

Herman, J. R., and J. E. Mentall, O_2 absorption cross sections (187–225 nm) from stratospheric solar flux measurements, *J. Geophys. Res.*, *87*, 8967–8975, 1982.

Holton, J. R., A dynamically based transport parameterization for one-dimensional photochemical models of the stratosphere, *J. Geophys. Res.*, *91*, 2681–2686, 1986.

Isaksen, I. S. A., and F. Stordal, Ozone perturbations by enhanced levels of CFCs, N_2O and CH_4: A two-dimensional diabatic circulation study including uncertainty estimates, *J. Geophys. Res.*, *91*, 5249–5263, 1986.

Jones, R. L., and J. A. Pyle, Observations of CH_4 and N_4O by the Nimbus 7 SAMS: A comparison with in situ data and two-dimensional numerical model calculations, *J. Geophys. Res.*, *89*, 5263–5279, 1984.

Kagann, R. H., J. W. Elkins, and R. L. Sams, Absolute band strengths of halocarbons F-11 and F-12 in the 8- to 16-μm region, *J. Geophys. Res.*, *88*, 1427–1432, 1983.

Keating, G. M., M. C. Pitts, G. Brasseur, and A. De Rudder, Response of middle atmosphere to short-term solar ultraviolet variations, 1, Observations, *J. Geophys. Res.*, *92*, 889–902, 1986.

Keeling, C. D., The global carbon cycle: What we know and could know from atmospheric, biospheric and oceanic observations, in *Proceedings of the Carbon Dioxide Research Conference: Carbon Dioxide Science and Consensus, Berkeley Springs, W. Va., September 19–23, 1982, CONF-820970, II.3–II.62*, U.S. Dep. of Energy, Washington, D. C., 1983.

Khalil, M. A. K., and R. A. Rasmussen, Increase and seasonal cycles of nitrous oxide in the earth's atmosphere, *Tellus*, *35B*, 161–169, 1983.

Kiehl, J. T., and V. Ramanathan, CO_2 radiative parameterization used in climate models: Comparison with narrow band models and with laboratory data, *J. Geophys. Res.*, *88*, 5191–5202, 1983.

Kiehl, J. T., C. Bruehl, and T. Yamamouchi, A parameterization for the absorption due to the near infrared bands of CO_2, *Tellus*, *37B*, 189–196, 1985.

Ko, M. K. W., M. B. McElroy, D. K. Weisenstein, and N. D. Sze, Lightning: A possible source of stratospheric odd nitrogen, *J. Geophys. Res.*, *91*, 5395–5404, 1986.

Kockarts, G., Absorption and photodissociation in the Schumann-Runge bands of molecular oxygen in the terrestrial atmosphere, *Planet. Space Sci.*, *24*, 589–604, 1976.

Kouker, W., and G. Brasseur, Transport of atmospheric tracers by planetary waves during a stratospheric warming event: A three-dimensional model simulation, *J. Geophys. Res.*, *91*, 13,167–13,185, 1986.

Lacis, A., J. Hansen, P. Lee, T. Mitchell, and S. Lebedeff, Greenhouse effects of trace gases, 1970–1980, *Geophys. Res. Lett.*, *8*, 1035–1038, 1981.

Liou, K.-N., and S.-C. S. Ou, Theory of equilibrium temperatures in radiative-turbulent atmospheres, *J. Atmos. Sci.*, *40*, 214–229, 1983.

Logan, J. A., M. J. Prather, S. C. Wofsy, and M. B. McElroy, Tropospheric chemistry: A global perspective, *J. Geophys. Res.*, *86*, 7210–7254, 1981.

Manabe, S., and R. T. Wetherald, Thermal equilibrium of the atmosphere with a given distribution of relative humidity, *J. Atmos. Sci.*, *24*, 241–259, 1967.

McClatchey, R. A., W. S. Benedict, S. A. Clough, D. E. Burch, R. F.

Calfee, K. Fox, L. S. Rothman, and J. S. Garing, AFCRL atmospheric absorption line parameters compilation, *Rep. TR0096*, Air Force Cambridge Res. Lab., Cambridge, Mass., 1973.

Nicolet, M., Aeronomic reactions of hydrogen and ozone, in *Mesospheric Models and Related Experiments*, edited by G. Fiocco, pp. 1–51, D. Reidel, Hingham, Mass., 1971.

Nicolet, M., Photodissociation of nitric oxide in the mesosphere and stratosphere: Simplified numerical relations for atmospheric model calculation, *Geophys. Res. Lett.*, *6*, 866–869, 1979.

Nordhaus, W. D., and G. W. Yohe, Future carbon dioxide emissions from fossil fuels, in *Changing Climate: Report of the Carbon Dioxide Assessment Committee*, pp. 87–153, National Academy Press, Washington, D. C., 1983.

Owens, A. J., C. H. Hales, D. L. Filken, C. Miller, J. M. Steed, and J. P. Jesson, A coupled one-dimensional radiative convective, chemistry-transport model of the atmosphere, 1, Model structure and steady state perturbation calculations, *J. Geophys. Res.*, *90*, 2283–2311, 1985.

Prinn, R. G., R. A. Rasmussen, P. G. Simmonds, F. N. Alyea, D. M. Cunnold, B. C. Lane, C. A. Cardelino, and A. J. Crawford, The atmospheric lifetime experiments, 5, Results for CH_3CCl_3 based on three years of data, *J. Geophys. Res.*, *88*, 8415–8426, 1983.

Quinn, T. H., K. A. Wolf, W. E. Mooz, J. K. Hammitt, T. W. Chesnutt, and S. Sarms, Projected use, emissions, and banks of potential ozone-depleting substances, *Rep. N-2282 EPA*, Rand Corp. Santa Monica, Calif., 1986.

Ramanathan, V., Radiative transfer within the earth's troposphere and stratosphere, A simplified radiative-convective model, *J. Atmos. Sci.*, *33*, 1330–1346, 1976.

Ramanathan, V., and R. E. Dickinson, The role of stratospheric ozone in the zonal and seasonal radiative energy balance in the earth-troposphere system, *J. Atmos. Sci.*, *36*, 1084–1104, 1979.

Ramanathan, V., R. J. Cicerone, H. B. Singh, and J. T. Kiehl, Trace gas trends and their potential role in climate change, *J. Geophys. Res.*, *90*, 5547–5566, 1985.

Ramanathan, V., L. Callis, R. Cess, J. Hansen, I. Isaksen, W. Kuhn, A. Lacis, F. Luther, J. Mahlman, R. Reck, and M. Schlesinger, Climate-chemical interactions and effects of changing atmospheric trace gases, *Rev. Geophys.*, *25*, 1441–1482, 1987.

Rasmussen, R. A., and M. A. K. Khalil, Global atmospheric distribution and trend of methylchloroform (CH_3CCl_3), *Geophys. Res. Lett.*, *8*, 1005–1007, 1981*a*.

Rasmussen, R. A., and M. A. K. Khalil, Atmospheric methane (CH_4); trends and seasonal cycles, *J. Geophys. Res.*, *86*, 9826–9832, 1981*b*.

Rasmussen, R. A., and M. A. K. Khalil, Atmospheric trace gases: Trends and distributions over the last decade, *Science*, *233*, 1623–1624, 1986.

Roberts, R. E., J. E. Selby, and L. M. Biberman, Infrared continuum absorption by atmospheric water vapor in the 8–12 μm window, *Appl. Opt.*, *9*, 2085–2090, 1976.

Rogers, C. D., and C. D. Walshaw, The computation of infrared cooling rate in planetary atmospheres, *Q. J. R. Meteorol. Soc.*, *92*, 67–92, 1966.

Russell, J. M., III, J. C. Gille, E. E. Remsberg, L. L. Gordley, P. L. Bailey, S. R. Drayson, H. Fischer, A. Girard, J. E. Harries, and W. F. J. Evans, Validation of nitrogen dioxide results measured by the Limb Infrared Monitor of the Stratosphere (LIMS) experiment on Nimbus 7, *J. Geophys. Res.*, *89*, 5099–5107, 1984.

Schoeberl, M. R., and D. F. Strobel, The zonally averaged circulation of the middle atmosphere, *J. Atmos. Sci.*, *35*, 577–591, 1978.

Simmonds, P. G., F. N. Alyea, C. A. Cardelino, A. J. Crawford, D. M. Cannold, B. C. Lane, J. E. Lovelock, R. G. Prinn, and R. A.

Rasmussen, The atmospheric lifetime experiment, 6, Results from carbon tetrachloride based on 3 years data, *J. Geophys. Res.*, *88*, 8427–8441, 1983.

Singh, H. B., L. J. Salas, H. Shigeishi, and E. Scibner, Atmospheric halocarbons, hydrocarbons, and sulfur hexafluoride, global distributions, source and sinks, *Science*, *203*, 899–903, 1979.

Solomon, S., R. R. Garcia, and F. Stordal, Transport processes and ozone perturbations, *J. Geophys. Res.*, *90*, 12,981–12,989, 1985.

Stolarski, R. S., and R. J. Cicerone, Stratospheric chlorine: A possible sink for ozone, *Can J. Chem.*, *52*, 1610–1615, 1974.

Stordal, F., and I. S. A. Isaksen, Ozone perturbations due to increases in N_2O, CH_4 and chlorocarbons: Two-dimensional time-dependent calculations, *Tellus*, in press, 1987.

Stordal, F., I. S. A. Isaksen, and K. Horntveth, A diabatic circulation two-dimensional model with photochemistry: Simulations of ozone and long-lived tracers with surface sources, *J. Geophys. Res.*, *90*, 5757–5776, 1985.

Thompson, A. M., and R. J. Cicerone, Atmospheric CH_4, CO and OH from 1860 to 1985, *Nature*, *321*, 148–150, 1986.

Tricot, C., and A. Berger, Modelling the response of temperature to changes in trace gases: a review with emphasis on the transient response, *Climate Dyn.*, *2*, 39–61, 1987.

U.S. Standard Atmosphere, *NOAA-S/T 76-1562*, Supt. of Doc., U.S. Govt. Print. Office, Washington, D. C., 1976.

Wang, W.-C., and G. Molnar, A model study of the greenhouse effects due to increasing atmospheric CH_4, N_2O, CF_2Cl_2, and $CFCl_3$, *J. Geophys. Res.*, *90*, 12, 971–12,980, 1985.

Wang, W.-C., Y. L. Yung, A. A. Lacis, T. Mo, and J. E. Hansen, Greenhouse effect due to man-made perturbation of trace gases, *Science*, 194, 685–690, 1976.

Wang, W.-C., D. J. Wuebbles, W. M. Washington, R. G. Isaacs, and G. Molnar, Trace gases and other potential perturbations to global climate, *Rev. Geophys.*, *24*, 110–140, 1986.

Weiss, R. F., The temporal and spatial distribution of tropospheric nitrous oxide, *J. Geophys. Res.*, *86*, 7185–7195, 1981.

World Meteorological Organization (WMO) National Aeronautics and Space Administration (NASA), Atmospheric ozone 1985, assessment of our understanding of the processes controlling its present distribution and change, report, Geneva and Washington D. C., 1986.

Wuebbles, D. J., Chlorocarbon emission scenarios: Potential impact on stratospheric ozone, *J. Geophys. Res.*, *88*, 1433–1443, 1983.

Wuebbles, D. J., F. M. Luther, and J. E. Penner, Effect of coupled anthropogenic perturbations on stratospheric ozone, *J. Geophys. Res.*, *88*, 1444–1456, 1983.

Wuebbles, D. J., M. C. McCracken, and F. M. Luther, A proposed reference set of scenarios for radiatively active atmospheric constituents, *Rep. DOE/NBB-066* U.S. Dep. of Energy, Washington, D. C., 1984.

Yamanouchi, T., Experimental study on the absorption properties of the near infrared atmospheric bands (in Japanese), Ph.D. thesis, 287 pp., Tohoku Univ., Sendai, Japan, 1977.

Yung, Y. L., M. B. McElroy, and S. C. Wofsy, Atmospheric halocarbons: A discussion with emphasis on chloroform, *Geophys. Res. Lett.*, *2*, 397–399, 1975.

G. Brasseur and A. De Rudder, Belgian Institute for Space Aeronomy, 3 Avenue Circulaire, 1180 Brussels, Belgium.